

TR-15  
1969



## **Research on the Morphology of Precipitation and Runoff in Texas**

R.A. Clark

---

**Texas Water Resources Institute**

---

**Texas A&M University**

RESEARCH PROJECT TECHNICAL COMPLETION REPORT

Project Number A-002-Tex

May 1965 -- June 1968

Agreement Numbers

14-01-0001-704, 14-01-0001-814

14-01-0001-989, 14-01-0001-1412

RESEARCH ON THE MORPHOLOGY OF PRECIPITATION AND  
RUNOFF IN TEXAS

Principal Investigator

Robert A. Clark

The work upon which this publication is based was supported in part by funds provided by the United States Department of the Interior, Office of Water Resources Research, as authorized under the Water Resources Research Act of 1964.

Technical Report No. 15  
Water Resources Institute  
Texas A&M University

February 1969

## ABSTRACT

This project has consisted of two distinct phases: (1) equipment modification and installation with associated collection and (2) analyses of data plus development of hydrologic techniques.

Errors inherent in the utilization of radar as a hydrologic sensor are discussed. It is shown that errors in the measurement of in-cloud liquid water content can be as much as 100 per cent. Similar results will be obtained in the measurement of rainfall rates by weather radar.

It is demonstrated that radar can be used quite effectively in the synthesis of hydrographs. In particular, the feasibility of using radar in streamflow forecasting has been tested for the Little Washita River in Oklahoma. The results were very encouraging.

Techniques for hydrograph synthesis are discussed. These have been combined with a stochastic model (which incorporates a sixth-order Markov chain) for rainfall-runoff simulation. The proposed model has been tested thoroughly and appears to hold promise as a forecasting tool.

A study was made of Hurricane Beulah which produced extremely heavy precipitation in south Texas and fostered an unprecedented number of tornadoes. The injection of dry air into the area northeast of the parent cyclone was apparently responsible for the extreme instability and development of a large number of tornadoes in that region.

Keywords -- river forecasting\*/ rainfall-runoff relationships\*/  
radar meteorology/ hydrograph analysis/ forecasting/  
stochastic processes\*/ Monte Carlo method/ hurricanes\*

## ACKNOWLEDGMENTS

The work upon which this report is based was supported in part by funds provided by the United States Department of the Interior, Office of Water Resources Research, as authorized under the Water Resources Research Act of 1964.

Assistance in securing data for various portions of the work was provided by Mr. M. A. Hartman, Agricultural Research Service, Chickasha, Oklahoma; Mr. K. E. Wilk and Dr. E. Kessler, III, National Severe Storms Laboratory, ESSA, Norman, Oklahoma; Mr. A. A. Fischbach, Jr., Geological Survey, Oklahoma City, Oklahoma; Messrs. R. W. Baird and W. G. Knisel, Jr., Agricultural Research Service, Riesel, Texas; and Mr. T. Twichell, Geological Survey, Austin, Texas.

The following individuals also contributed both time and effort in the preparation of various portions of this study: Messrs. Jake Canglose and Gary K. Grice, Drs. Robert C. Runnels, James R. Scoggins, and Michael D. Hudlow, Captains John P. Huddle, Larry R. Heaton, and Odell M. Johnson, and Major Walter M. Dale.

The original and final manuscripts were typed by Mrs. Jan Bailey and Mrs. Nelda Taylor.

## TABLE OF CONTENTS

	Page
ABSTRACT . . . . .	ii
ACKNOWLEDGMENTS . . . . .	iii
LIST OF TABLES . . . . .	vi
LIST OF FIGURES . . . . .	vii
GENERAL . . . . .	1
EQUIPMENT PHASES. . . . .	1
Equipment Modification. . . . .	1
Hydrologic Equipment Purchase and Installation. . . . .	1
ERROR ANALYSIS . . . . .	6
Instrumental Accuracy . . . . .	6
Liquid-water content . . . . .	6
Vertical speed . . . . .	7
Meaning of the Estimates of the Error . . . . .	10
A CASE STUDY USING WEATHER RADAR . . . . .	12
Moisture Field . . . . .	12
Field of Vertical Speeds. . . . .	16
Summary of the Case Study . . . . .	18
HYDROGRAPH SYNTHESIS . . . . .	20
General . . . . .	20
Techniques Employed . . . . .	20
Hydrograph synthesis with the Pearson type III function . . . . .	21
Hydrograph synthesis by runoff routing . . . . .	29
An Example. . . . .	32
STREAMFLOW FORECASTING. . . . .	34
General . . . . .	34
Success of Runoff Prediction. . . . .	34
Comparison of Lag-Time Estimates. . . . .	36
Stochastic Model for Rainfall-Runoff Simulation . . . . .	38
Rainfall model . . . . .	38

	Page
Rainfall-runoff simulation. . . . .	49
Testing rainfall synthesis by Monte Carlo methods . .	50
Comparison of conditional probabilities . . . . .	69
HURRICANE BEULAH . . . . .	78
General. . . . .	78
Tornadoes Associated with Beulah. . . . .	80
Daily and areal distributions . . . . .	82
Possible Course of the Tornadoes . . . . .	86
Conclusions. . . . .	88
TABLES OF PRECIPITABLE WATER AND VERTICAL VARIATION OF TEMPERA- TURE . . . . .	88
APPENDIX A PROJECT RELATED REPORTS, PUBLICATIONS, AND PAPERS. .	92
REFERENCES . . . . .	94

LIST OF TABLES

Table	Page
1. Summary of errors of w . . . . .	10
2. Storage coefficients for the Little Washita . . . . .	32
3. Average precipitation and runoff derived from various rainfall measurements compared to each other and to ob- served values . . . . .	35
4. Lag times and peak discharges derived from various rain- fall measurements compared to observed values . . . . .	37
5. Classes of hourly amounts of rainfall and mean rainfall for the classes. . . . .	43
6. First order transitional probabilities for synoptic type 3 (stationary front) . . . . .	45
7. Transitional probabilities for the secondary position of the Markov chain . . . . .	47
8. Complete scheme for the sixth-order Markov chain . . . . .	48
9. D and $\chi^2$ values of selected characteristics of rainfall sequences for type 1 (cold front) storms . . . . .	65
10. Percentage of storms passing the Mann-Whitney U Test at a significance level of 0.01 . . . . .	66
11. Percentage of storms passing the Wald-Wolfowitz runs test at a significance level of 0.05 . . . . .	67
12. Number of gages used and corresponding gage densities . .	72
13. Classes of amounts of hourly precipitation . . . . .	74
14. Results of $\chi^2$ test of frequency distributions . . . . .	76
15. Depth of precipitable water (mm) between 1000-mb surface and indicated height (m) above 1000-mb as a function of 1000-mb temperature (C) in a saturated atmosphere with pseudoadiabatic lapse rate . . . . .	90
16. Temperature (C) as a function of height (meters) above 1000-mb temperature at 1000-mb in a saturated atmosphere with a pseudoadiabatic lapse rate . . . . .	91

## LIST OF FIGURES

Figure	Page
1. The console of the 3.2-cm, CPS-9 radar . . . . .	2
2. The rebuilt console of the 10.3-cm, TAM-1 radar. . . . .	2
3. East Yegua Basin near Dime Box, Texas . . . . .	4
4. Burton Creek Watershed -- Bryan, Texas . . . . .	5
5. Time-height cross section of liquid-water concentration for the core of Echo 3 . . . . .	13
6. Histogram of the percentage of observations of liquid- water concentration that are contained in the class intervals indicated on the abscissa . . . . .	15
7. Time-height cross section of the vertical speeds for the core of Echo 3 . . . . .	17
8. Percentage of observation of updrafts measured at 11,000 ft . . . . .	19
9. Map of Little Washita River basin with insert showing location in Oklahoma . . . . .	22
10. Isochrones for the Little Washita (hr) . . . . .	27
11. Comparison of synthesized hydrographs to the observed hydrograph for the storm of May 9, 1965. Little Washita River nr. Ninnekah, Oklahoma . . . . .	33
12. Average correlogram of hourly rainfall at Ninnekah, Oklahoma . . . . .	40
13. Transition probabilities follow dry periods . . . . .	46
14. Frequency histogram of hydrograph-peak discharges, as de- rived from the stochastic model (storm of May 9, 1965, 1st two hours of rainfall given) . . . . .	51
15. Bar graph of hourly rainfall illustrating wet period lengths. . . . .	52
16. Map of Lowery Draw Watershed . . . . .	70
17. Single (dashed line) and 14 rain-gage (solid line) distri- butions of conditional probabilities for all precipitation types . . . . .	77
18. Total precipitation (inches), September 19-September 23, 1967 . . . . .	81
19. Relation of tornado occurrence to time of the day . . . . .	84



## RESEARCH ON THE MORPHOLOGY OF PRECIPITATION AND RUNOFF IN TEXAS

### GENERAL

This project might be characterized as consisting of two distinct phases: (1) equipment modification and installation with associated data collection and (2) analyses of data plus development of hydrologic techniques. A list of reports, publications, and papers presented is given in Appendix A. Although techniques developed during this study were based primarily on data collected in Texas and Oklahoma, they should be equally applicable to other areas. In this report only basic results will be summarized, for a more detailed discussion the reports listed in Appendix A should be consulted.

### EQUIPMENT PHASES

#### Equipment Modification

A dual-frequency radar system (3.2- and 10.3-cm radars) was developed in the Department of Meteorology, Texas A&M University, during the period 1960-1965 under two grants from the National Science Foundation. Except for the wavelength of transmission, the two radars had nearly identical characteristics. The only real difference was in the consoles on which radar data were displayed. Under Project A-002-Tex new Plan Position Indicator (PPI) and Range Height Indicator (RHI) scopes were purchased in 1966 to replace equipment in use at that time. These scopes, coupled with parts cannibalized from a surplus CPS-9 radar purchased in 1965, were utilized in a remodeling program to rebuild completely the 10.3-cm radar display, Figs. 1 and 2. This modification, which was completed in May 1967, increased greatly the compatibility of the dual-frequency system.

#### Hydrologic Equipment Purchase and Installation

The feasibility of using radar data in hydrologic studies can best be tested when compared with actual rainfall and runoff data. As a result, a search was made for a relatively small basin within 30 to 75 mi of Texas A&M University on which the streamflow was being gaged

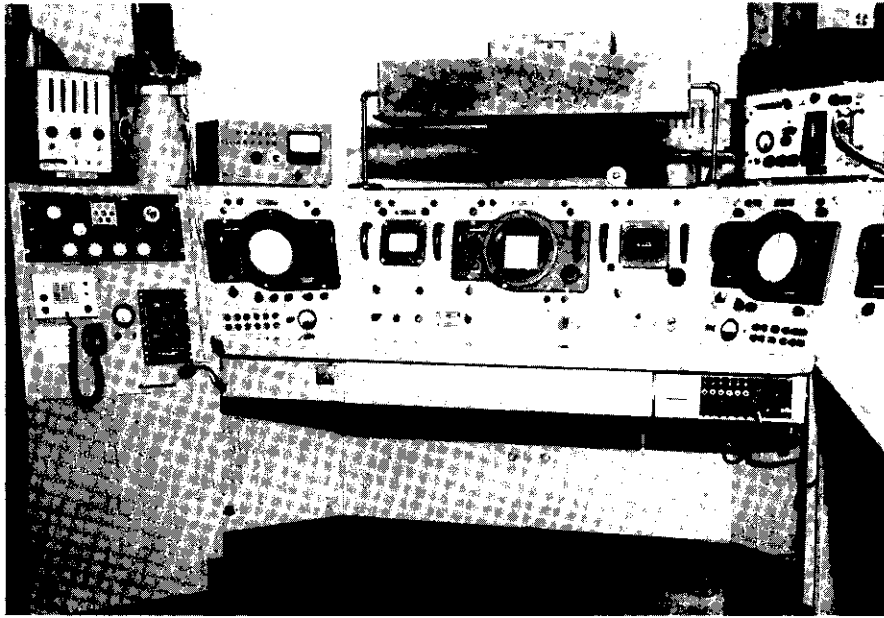


Figure 1. The console of the 3.2-cm, CPS-9 radar. The RHI and PPI scopes have been switched from the standard display.

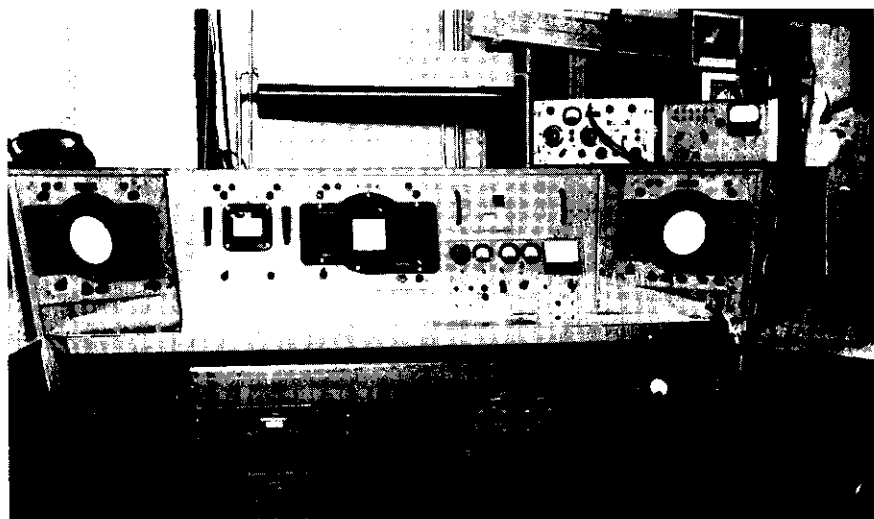


Figure 2. The rebuilt console of the 10.3-cm, TAM-1 radar. Note that the display is now identical to the CPS-9 radar.

currently by the Geological Survey, U.S. Department of Interior. The most favorable direction for operation of the Texas A&M University radar system was to the west. The East Yegua Creek basin located approximately 35 mi west of Texas A&M University came closest to fulfilling our requirements. That basin has been gaged by the Geological Survey since 1962 and has a drainage area of 243 mi<sup>2</sup>. Ten recording and 20 non-recording rain gages were purchased and installed within the basin. The location of the gages is shown in Fig. 3. All of the stations are operated by cooperating ranchers and farmers. The entire system was completed in the spring of 1966. Over two years of data have now been collected. Data from this network will continue to be collected under Project Themis; that project, sponsored by the Department of Defense, will continue the collection of data by the radar system and relate it to hydrologic data for morphological studies of rainfall and runoff.

In addition, under Project Themis, two micrometeorological stations providing information on low level winds, temperature, humidity, radiation, and soil temperature have been installed in the East Yegua Creek basin. Coupled with the already established rain-gage network, it is anticipated that valuable information on meso- and micro-scale variations in atmospheric parameters can be obtained.

A second network of 36 non-recording rain gages was established over the Burton Creek drainage basin located in the City of Bryan, Texas. Fig. 4 presents the network established over this 7 mi<sup>2</sup> basin. A cooperative program between the Geological Survey and Texas A&M University has established a stream gage which measures flow from a sub-area, 1.46 mi<sup>2</sup>, of the Burton Creek basin. The establishment of the stream gage in May 1968 was somewhat fortuitous in that over 25 in. of rain were observed in the Water Resources Institute (WRI) network during May and June 1968. Data from this network will be used in studies related to the areal variation of rainfall over small areas. These data will be used also in conjunction with the streamflow data to study runoff characteristics from an urban drainage basin.

The runoff and rainfall data from the small watershed will be utilized also in connection with Project A-010-Tex which is an investiga-

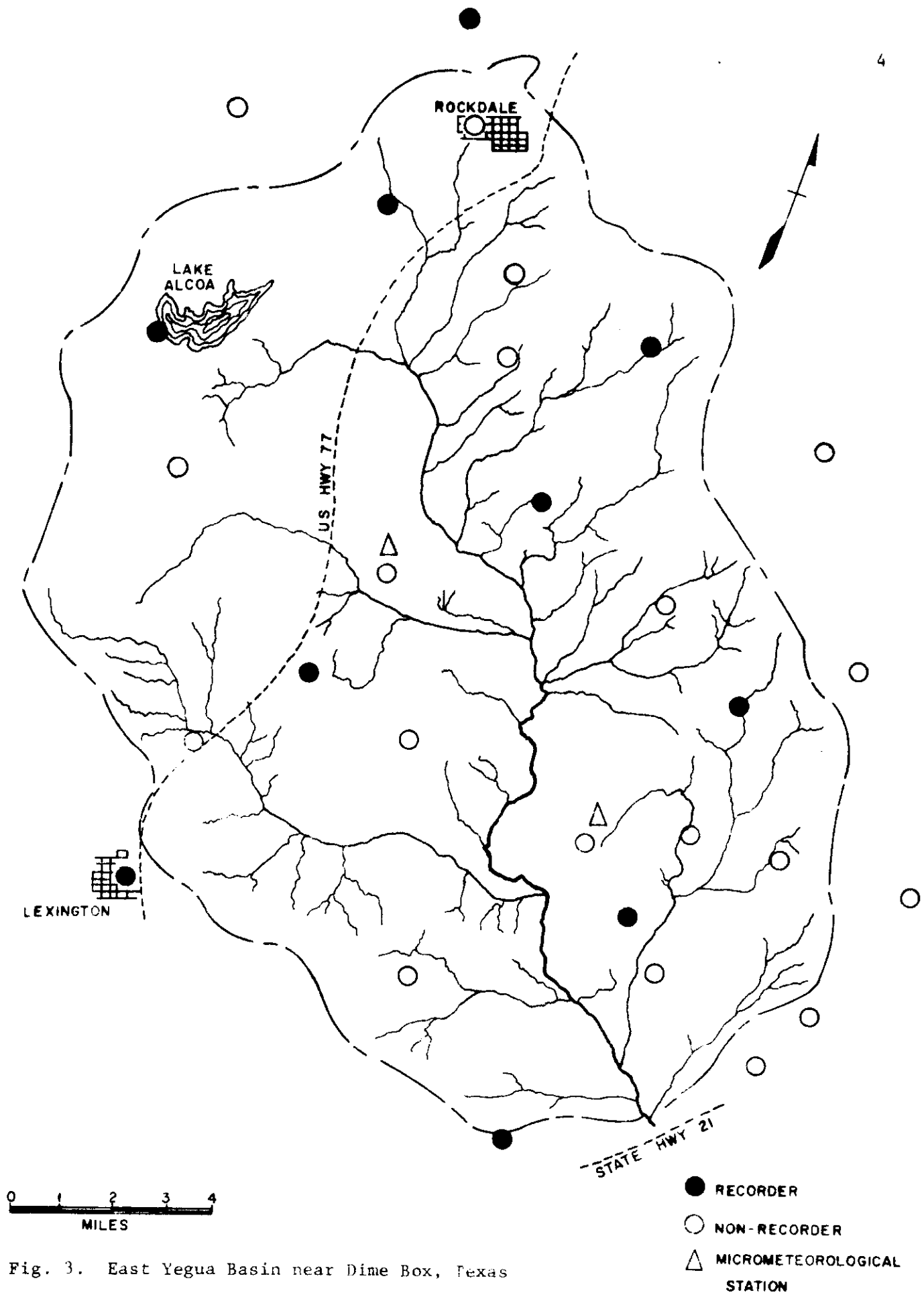


Fig. 3. East Yegua Basin near Dime Box, Texas

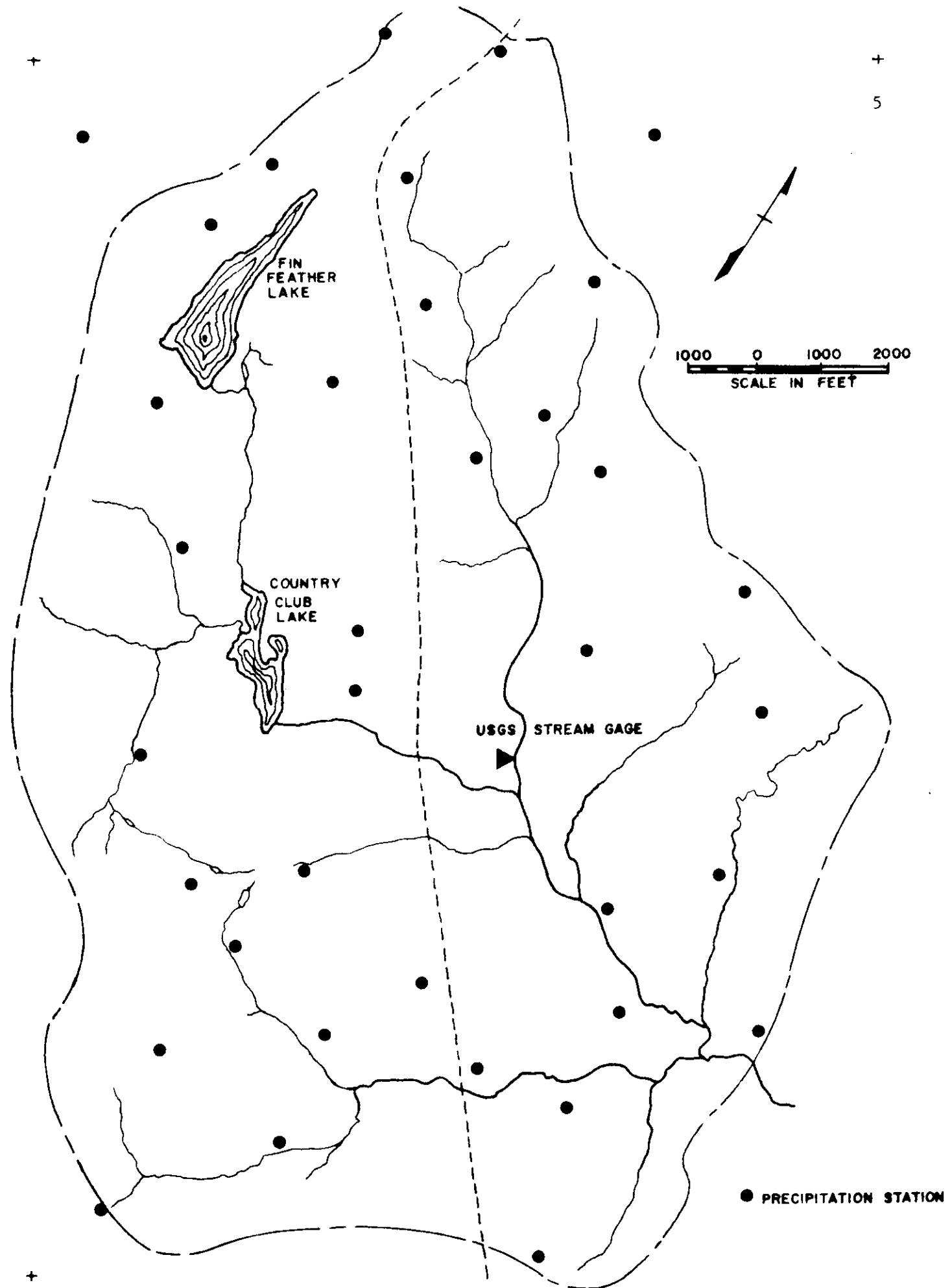


Fig. 4. Burton Creek Watershed - Bryan, Texas.

tion of a linear model to describe hydrologic phenomenon of drainage basins. These data will serve as a check on the proposed model.

## ERROR ANALYSIS

### Instrumental Accuracy

Liquid-water content. Weather radar has the capability of mapping fields of liquid-water or solid-water concentration, regions of disturbed refractive-index gradient, and solid objects in the atmosphere such as birds and aircraft. From a hydrologic point-of-view, regions of the atmosphere containing hydrometers which may produce "rain" at the surface of the earth are of primary importance. A study by Runnels (1967) related to instrumental accuracy was performed to estimate the errors in the measurement of liquid-water concentration by weather radar.

The liquid-water content for a point within a cloud can be shown to be related approximately to the average power received by the weather radar by the expression

$$M = 3.94 \times 10^{-3} \left[ \frac{\bar{P}_r r^2}{C_1 K^2} \right]^{0.55}, \quad (1)$$

where  $M$  is the liquid water content in  $\text{gm m}^{-3}$ ,  $\bar{P}_r$  is the average received power in  $\text{mw}$ ,  $r$  is the range in  $\text{st mi}$ ,  $C_1$  is a radar constant with units of  $\text{mw mi}^2 \text{m}^3 \text{mm}^{-6}$ , and  $K^2$  is a dielectric factor used in Rayleigh scattering theory. Experimental work has shown that this equation probably underestimates the liquid-water content because of an inexact description of the radar beam. A reasonable estimate of the uncertainty can be made if  $C_1$  is determined from the version of the radar equation derived by Probert-Jones (1962). Using his expression for  $C_1$  and assuming Rayleigh scattering, the systematic underestimate of  $M$  can be accounted for by increasing the measured values of  $\bar{P}_r$  by 1.4 db.

The determination of the total error of  $M$  was based on the Methodology that is variously called "compounding of errors" (Wilson, 1952) or "propagation of errors" (Beers, 1957). Each term in Eq. 1 was examined and its contribution to the total error in  $M$  determined. The errors of the received power and the radar constant were the largest contributors

to the error of M. In particular, the uncertainty arising from use of the gain-step method is the greatest. The fractional error in M,  $S_M$ , was determined to be 1.024 (102.4 per cent), about 2 db.

Since rain at the surface must be inferred from these liquid-water fields, which are measured aloft, it is apparent that large errors in rainfall rate may result from radar measurements.

The equation that is generally applied in determination of rainfall rates is

$$Z = AR^B, \quad (2)$$

where Z is the reflectivity factor which can be obtained from radar measurements of received power, A and B are constants which are dependent upon the rainfall type (and other climatic factors), and R is the rainfall rate. Scattering theory indicates that Z is dependent upon the summation of drop diameters to the sixth power while the liquid-water content, M, of the atmosphere is related to drop diameters to the third power. The rainfall rate, R, is related also to drop diameters to the third power. Thus, it seems reasonable to assume that errors incurred in the measurement of M will result in similar errors in R. The study by Runnels was concerned primarily with errors related to instrumental design and not to false indications due to other atmospheric factors. Greene et al. (1966) demonstrated that very large errors in R, which are not related to instrumental design, might occur due to vertical motion in the atmosphere. Although the work of Runnels tends to discourage the use of weather radar for the measurement of rainfall intensity, the studies of Hudlow (1967) demonstrate the feasibility of utilizing radar measurements, particularly estimates of the areal distribution of rainfall, for streamflow forecasting.

Vertical speed. The rate of formation and subsequent development of rain in moist air is very closely related to the three-dimensional winds affecting the regime of formation. Kessler (1959) has suggested the use of a continuity equation for water substance to gain insight into changes in cloud parameters. This equation was used by Runnels (1967) to calculate vertical speeds in convective clouds. The results of these calculations were reasonable ones for the cumulus congestus clouds that were studied and are presented later in this report.

The average vertical speed,  $w$ , can be shown to be related to the rate of change and vertical gradient of  $M$  by

$$W = \frac{\frac{\Delta M}{\Delta t} + M \frac{\overline{\Delta V}}{\Delta z} + \overline{V} \frac{\Delta M}{\Delta z} - \tau}{M \frac{\Delta \ln \rho}{\Delta z} - \frac{\Delta M}{\Delta z}}, \quad (3)$$

where  $\overline{V}$  is the speed of the drop with median-volume diameter,  $z$  is the vertical Cartesian space coordinate,  $\rho$  is the air density,  $t$  is time, and  $\tau$  is a coalescence-transfer term. The fractional error of the vertical speed,  $w$ , is equal to the square root of the sum of the squares of the fractional errors of the terms on the right-hand side of Eq. 3. Therefore, the fractional error of  $w$ ,  $S_w$ , is given by

$$S_w = (S_1^2 + S_2^2 + S_3^2 + S_4^2 + S_5^2 + S_6^2)^{\frac{1}{2}}, \quad (4)$$

where the subscripts 1 through 6 refer to the terms on the right-hand side of Eq. 3. The numbering proceeds from left to right in the numerator and then from left to right in the denominator. Thus the error of  $M(\Delta \ln \rho / \Delta z)$  is designated by  $S_5$ .

The method of calculating the fractional error of the terms in Eq. 3 was similar for each of the terms since all but one is expressed as a ratio. We will show the development of the error of  $\Delta M / \Delta t$  and simply state the calculated errors of the remaining terms.

The error of  $\Delta M / \Delta t$ ,  $S_1$ , is

$$S_1 = (S_{\Delta M}^2 + S_{\Delta t}^2)^{\frac{1}{2}}, \quad (5)$$

where  $S_{\Delta M}$  is the error of  $\Delta M$  and  $S_{\Delta t}$  is the error of  $\Delta t$ . The error of time increment was very small since the clock used to measure time varied only in a slow systematic manner. The absolute error of  $\Delta M$ ,  $s_{\Delta M}$ , is related to the absolute error of  $M$ ,  $s_M$ , by

$$s_{\Delta M}^2 = 2 s_M^2. \quad (6)$$

The absolute error of  $M$  may be expressed as

$$s_M = S_M M, \quad (7)$$



where  $M$  is evaluated at the center of the difference  $\Delta M$ . Elimination of  $s_M$  between Eqs. 6 and 7 gives

$$s_{\Delta M}^2 = 2 S_M^2 M^2, \quad (8)$$

and division by  $(\Delta M)^2$  yields

$$S_{\Delta M}^2 = 2 S_M^2 \left(\frac{M}{\Delta M}\right)^2. \quad (9)$$

Eq. 9 shows that the fractional error of  $\Delta M$  depends on the time and location in the cloud at which  $M$  and  $\Delta M$  are measured. To determine an upper limit of  $S_{\Delta M}$ , it was decided to choose a value of  $M$  corresponding to a reasonably-large value that could be expected in the clouds which were studied. The summary of the maximum values of liquid-water content that is given in the text by Fletcher (1962) was used to ascertain this large value. A value of  $2.0 \text{ gm m}^{-3}$  appeared to be an average of the various maxima that appeared in the summary. For a value of  $\Delta M$  to be used in Eq. 9 we decided to use a small, yet representative, value of  $\Delta M$  in order to obtain a value of the error which is unlikely to be exceeded by any one measurement. A value of  $0.3 \text{ gm m}^{-3}$  appeared to be a typical minima of the values calculated during a case study using the TAM-1 radar. Substitution of the above-mentioned values for  $S_M$ ,  $M$  and  $\Delta M$  into Eq. 9 gives

$$\begin{aligned} S_{\Delta M} &= 9.34 S_M \\ &= 9.564, \end{aligned} \quad (10)$$

which is the same as the fractional error  $S_1$ .

The error of  $M(\overline{\Delta V}/\Delta z)$  and other terms was determined in a manner which is similar to the method used above. Eq. 4 then was used to compute the total error of  $w$ . The values of the partial errors were substituted for the terms on the right-hand side of the equation. Table 1 summarizes the calculation of the error of  $w$ . The fractional error of  $w$ , therefore, is estimated to be  $\pm 13.787$  (a percentage error of  $\pm 1378.7\%$ ) and the error in decibels is  $\pm 11.39$  db.

Reduction of this error would require reductions in the error of  $M$  since the error of the measurements of liquid-water content is the largest contributor to the error of  $w$ .

Table 1. Summary of errors of w

Term	Error	Square of error
$\frac{\Delta M}{\Delta t}$	9.564	91.470
$\frac{-\Delta M}{V \Delta z}$	1.024	1.048
$M \frac{\Delta \bar{V}}{\Delta z}$	1.024	1.048
$\tau$	2.000	4.000
$M \frac{\Delta(\ln \rho)}{\Delta z}$	1.024	1.048
$\frac{\Delta M}{\Delta z}$	9.564	91.470
	Total	190.084
Square root of total =		13.787

#### Meaning of the Estimates of the Error

The previous discussions of the estimated limits of the errors of M and w have considered quantitative measures of these uncertainties, but a precise meaning of the error limits was not considered. The following discussion is presented concerning the nature of the experimental error.

Semi-objective estimates were made of the error limits of the parameters which appeared in the basic equations. These estimates are termed semi-objective since they represent estimates that were not determined with a degree of accuracy necessary for a rigorous analysis of the experi-

mental errors. However, it was felt that these estimates were the best available and that the magnitudes were reasonable ones.

Before assigning a specific meaning to these semi-objective estimates, we will consider the nature of the observations which determine the form of the quantity used to express the limits of error. These forms are based on the assumption that successive observations of the same quantity should be distributed in a random sequence. It is considered that there exists a hypothetical population made up of the results which would be obtained if the given observation were repeated a very large number of times.

Any single observation or set of observations is regarded as a random sample from this population. The usual assumption which is made concerning the random errors is that they are distributed according to the Gauss or "normal" law of error. This law appears to be qualitatively correct since repeated observations of a single quantity support the idea of a continuous distribution with a single maximum and a monotonic falling off toward zero on either side. In addition, such curves generally appear to be symmetrical. In practice, the number of measurements of a given quantity may be quite small and the available data may or may not be distributed in a manner approximating the normal law. This situation prevailed in this investigation. Only a single measurement could be performed before the fluctuating motion inside a cloud would change the experimental conditions. Thus we lacked information either to confirm or reject the assumption that the semi-objective estimates of the radar parameters and the cloud parameters would be distributed normally if a sufficient number of measurements could be performed. However, since repeated measurements of many physical quantities are distributed normally, we decided to make the assumption that the measured values and estimates of these parameters were random samples from a population which satisfied the normal law of error. This assumption allowed us to be more exact in the specification of the limits of error since we could employ the statistics of a normally-distributed variable.

When observational data are distributed normally two measures of dispersion that are in common use are the standard deviation (S.D.) and the probable error (P.E.). If  $\bar{M}$  represents a particular value of the

liquid-water content which has been measured by the radar, then the interval  $\bar{M} \pm S.D.$  will cover the most probable value of  $M$  in 68.3 per cent of the cases, in the long run. Similarly, the interval  $\bar{M} \pm P.E.$  will contain the most probable value of  $M$  in 50.0% of the cases. If as we have assumed, the population of random errors is normally distributed, then

$$P.E. = 0.674 S.D. \quad (11)$$

Griffiths (1967) has stated his experience led him to conclude that such semi-objective estimates of errors, when made by competent observers, are probably the limits that will not be exceeded nine times out of ten. If we assume that the absolute errors (designated by  $s$ ) which have been computed in this chapter are the 0.90 confidence limits, then the most probable value of the variable of interest (say  $M$ ) will be found in the interval  $\bar{M} \pm s$  in 90% of the cases. Again, if the population of random errors is normally distributed, then

$$s = 1.645 S.D. \quad (12)$$

Based on the Griffiths' conclusion, it seemed reasonable to stipulate that the experimental errors of both the component and compounded terms were the limits which would not be exceeded nine times out of ten, in the long run.

#### A CASE STUDY USING WEATHER RADAR

Twenty-three separate clouds were studied during July 1967 with reference to liquid-water content and vertical motion. The results of each varied from echo to echo. However, it was possible to discern features which were common to the whole class of echoes. In this section the results of the analyses of the moisture fields and field of vertical speeds are presented.

##### Moisture Field

The moisture field for Echo 3 is presented in Fig. 5. The initial phases of the cycle were characterized by an increase of liquid water as the updrafts supplied vapor and condensed water. As soon as the drops were of sufficient size to produce a radar echo, a downward extension of

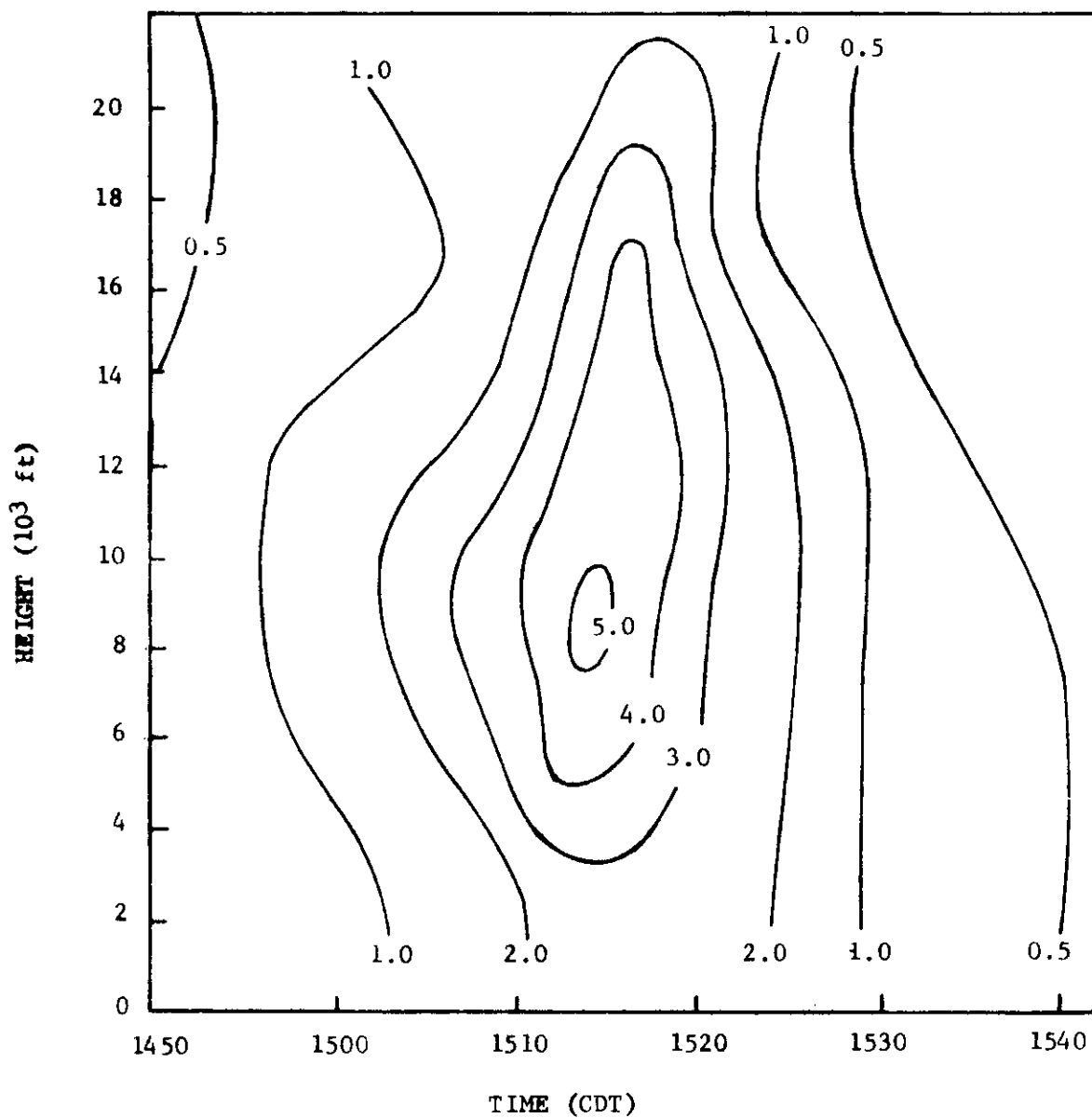


Fig. 5. Time-height cross section of liquid-water concentration for the core of Echo 3. Isopleths of liquid-water concentration are in gm m<sup>-3</sup>.

the echo was noted. This extension was interpreted to be the result of the drag-induced downdraft and the coalescence mechanism which produced radar-detectable drops as coalescences occurred. The base of this cloud was estimated to be 5000 ft MSL, which was the convective condensation level.

Fig. 5 is typical of the time-height cross sections which were constructed for each of the other echoes studied during this investigation. Each pattern was essentially symmetrical with time, indicating a cyclical increase of moisture that was followed by a decrease as the cloud passed to the dissipating stage. Another characteristic of each echo was the increase of liquid water with height until a maximum was attained.

In spite of the large error of  $M$  that was estimated previously, we felt that the form of Fig. 5 was qualitatively correct since the pattern is reasonable for a convective cell undergoing cyclic development. The point measurements of  $M$  that were used to construct this cross section may have fractional errors as large as 100 per cent at the 0.90 level of confidence. The construction of scalar fields from these point measurements introduced a smoothing which produced a field that was qualitatively reasonable. Reduction of the experimental error would produce a pattern that would have a similar shape but the reliability of such a pattern would be much higher.

Some of the values of liquid-water concentration that are shown in Fig. 5 are comparable to those reported by other investigators (Fletcher, 1962 and Byers, 1965). However, when all of the echoes were considered some rather large values of liquid-water content appeared. The 695 point measurements from all of the echoes were grouped and the frequencies were plotted to show the variation of these data. Fig. 6 shows the results of this grouping.

Measurements of liquid-water content that have been made from instrumented aircraft generally show that average values range from approximately 0.10 to 1.50  $\text{gm m}^{-3}$  (Fletcher, 1962). These same sources report maximum values ranging from approximately 0.20 to 3.50  $\text{gm m}^{-3}$  with means of about 1.50  $\text{gm m}^{-3}$ . The mean of the data presented in Fig. 6 is 2.17  $\text{gm m}^{-3}$ .

Certainly, not all the individual measurements which comprise the data of Fig. 6 can be interpreted as average values of liquid-water content.

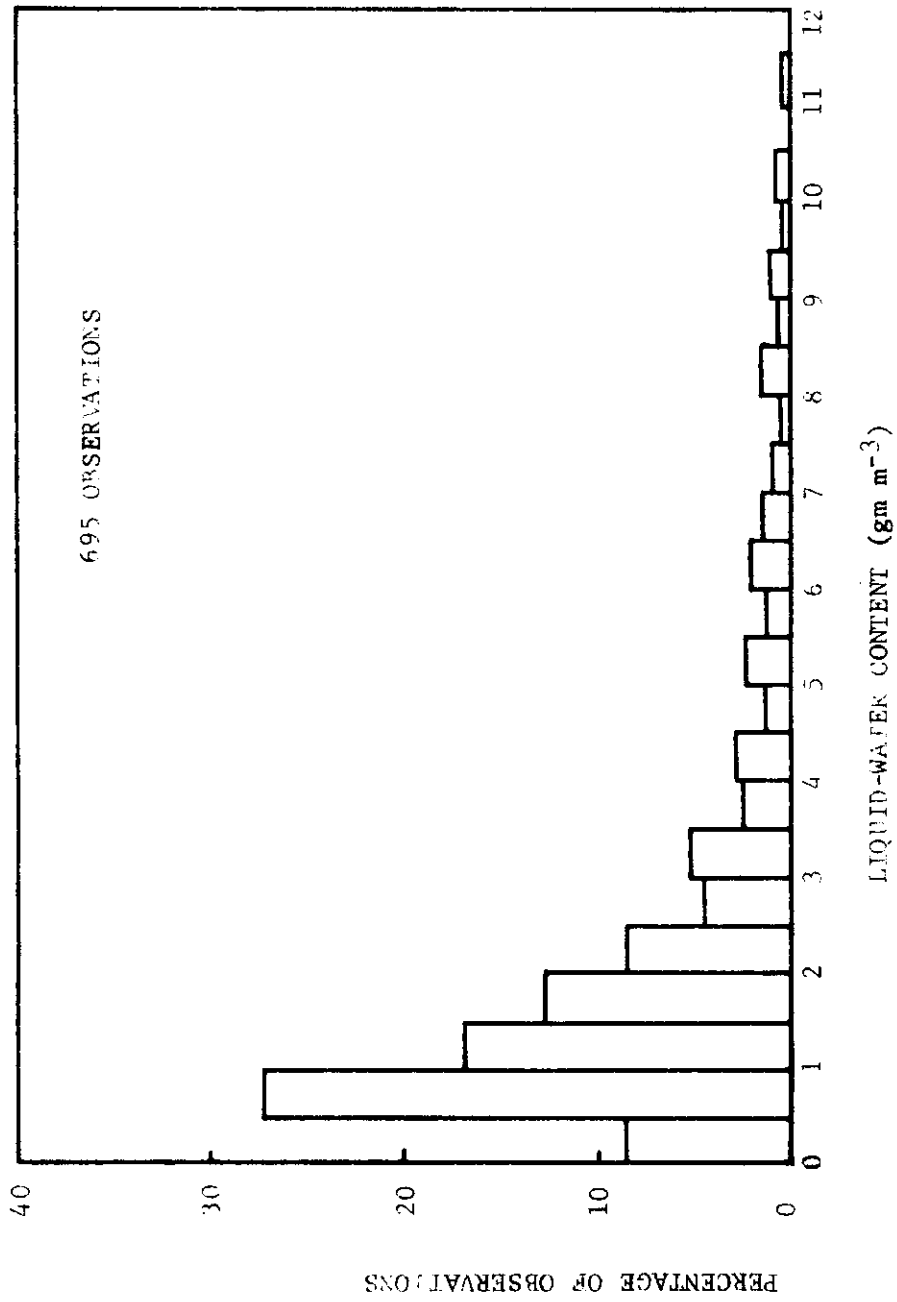


Fig. 6. Histogram of the percentage of observations of liquid-water concentration that are contained in the class intervals indicated on the abscissa.

Some represent values corresponding to measurements made early and late in the cycle of the convective cell when values might be less than average and some of the measurements were made at times when maximum concentrations of liquid-water content were being observed. Thus, some caution must be exercised in comparing the values reported in the literature and the radar-measured values. However, the fact that the mean of all observations was 1.45 times the mean of the maxima as measured by aircraft would indicate that an experimental uncertainty which was of the order of one was vitiating the results.

Although it is desirable to obtain values of the liquid-water content whose magnitudes are physically reasonable, it is equally important that the spatial and temporal pattern of these measured quantities also be physically meaningful. Point values of  $M$  must be related to other values in the neighborhood of the point in question. With an experimental error as large as that estimated for the apparatus used in this study, both the magnitudes and the variations of these magnitudes with distance and time may be atypical. We noted previously, however, that the fractional error of one did not seem to change appreciably the gross features of the fields of  $M$ .

The form of the moisture field associated with the core of Echo 3 is very similar to that of the idealized convective cloud described by Byers and Braham (1949). They described the life cycle of a large convective cloud as consisting of three distinct stages of development. These are: a cumulus stage, characterized by updrafts throughout the cell; a mature stage, characterized by both updrafts and downdrafts, at least in the lower half of the cell; and a dissipating stage, characterized by weak downdrafts prevailing throughout the cell.

#### Field of Vertical Speeds

The time-height cross section of the vertical speeds at the core of Echo 3 is presented in Fig. 7 and it contains some values that are quite unrealistic when compared to updrafts and downdrafts measured in such investigations as the Thunderstorm Project (Byers and Braham, 1949). Time-height cross sections of vertical speeds were constructed for each of the 23 echoes which were studied. In many of these cross sections very large



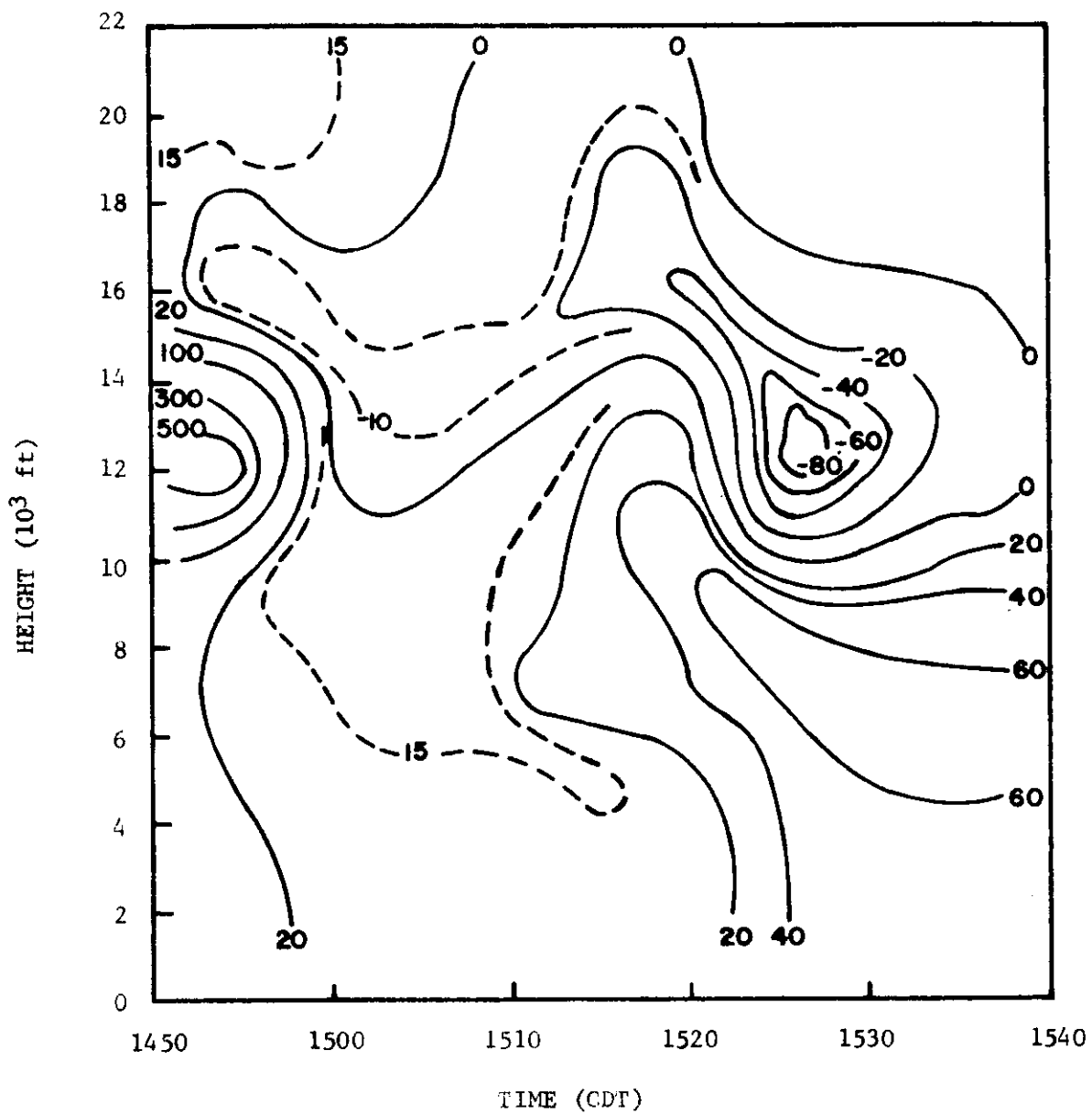


Fig. 7. Time-height cross section of the vertical speeds for the core of Echo 3. Isopleths of vertical speeds are in  $\text{m sec}^{-1}$ .

values of both positive and negative speeds were encountered. Each of the cross sections was similar to Fig. 7, that is, the analyzed fields of vertical speeds contained values of vertical speeds that were reasonable, but the presence of unrealistic updrafts and/or downdrafts produced fields with little physical meaning or any systematic patterns comparable to the idealized cell of Byers and Braham. In order to achieve an over-all picture of these large updrafts and downdrafts, we decided to group the various vertical speeds. Percentage polygons of the updrafts computed from the continuity equation were constructed for altitudes of 5, 11, 16, and 20 thousand feet above mean sea level. Fig. 8 presents the results for 11,000 MSL ft. The heights were selected to correspond to frequency distributions appearing in the report of the Thunderstorm Project. The percentage polygons representing the data from the Thunderstorm Project are shown as dashed lines in the Fig. 8. Similar polygons were constructed for the downdrafts. Several extreme values of vertical speeds were not shown in these figures because of the scale which was chosen.

When we considered the large error of  $w$  that was estimated previously, it was easy to see how extreme values can arise as well as the speeds whose values fell in the class intervals between 30 and 100  $\text{m sec}^{-1}$ . In some instances the vertical speeds measured by radar that were less than, say, 25  $\text{m sec}^{-1}$  were in good agreement with the data from the Thunderstorm Project. This agreement was not completely unsuspected since some of the radar-measured values of  $w$ , even with the large experimental error, were expected to agree with what may be termed "the more probable speeds" of the Thunderstorm Project. As in the case of the fields of liquid-water content, these large uncertainties in  $w$  have produced spatial and temporal patterns that are not typical.

#### Summary of the Case Study

Point values of liquid-water content were measured at the core of 23 convective clouds that formed near College Station, Texas. Scalar fields of liquid water were constructed for each cloud. The gross features of these fields appeared to be physically reasonable one, but the large experimental error inherent in the technique and apparatus caused certain point

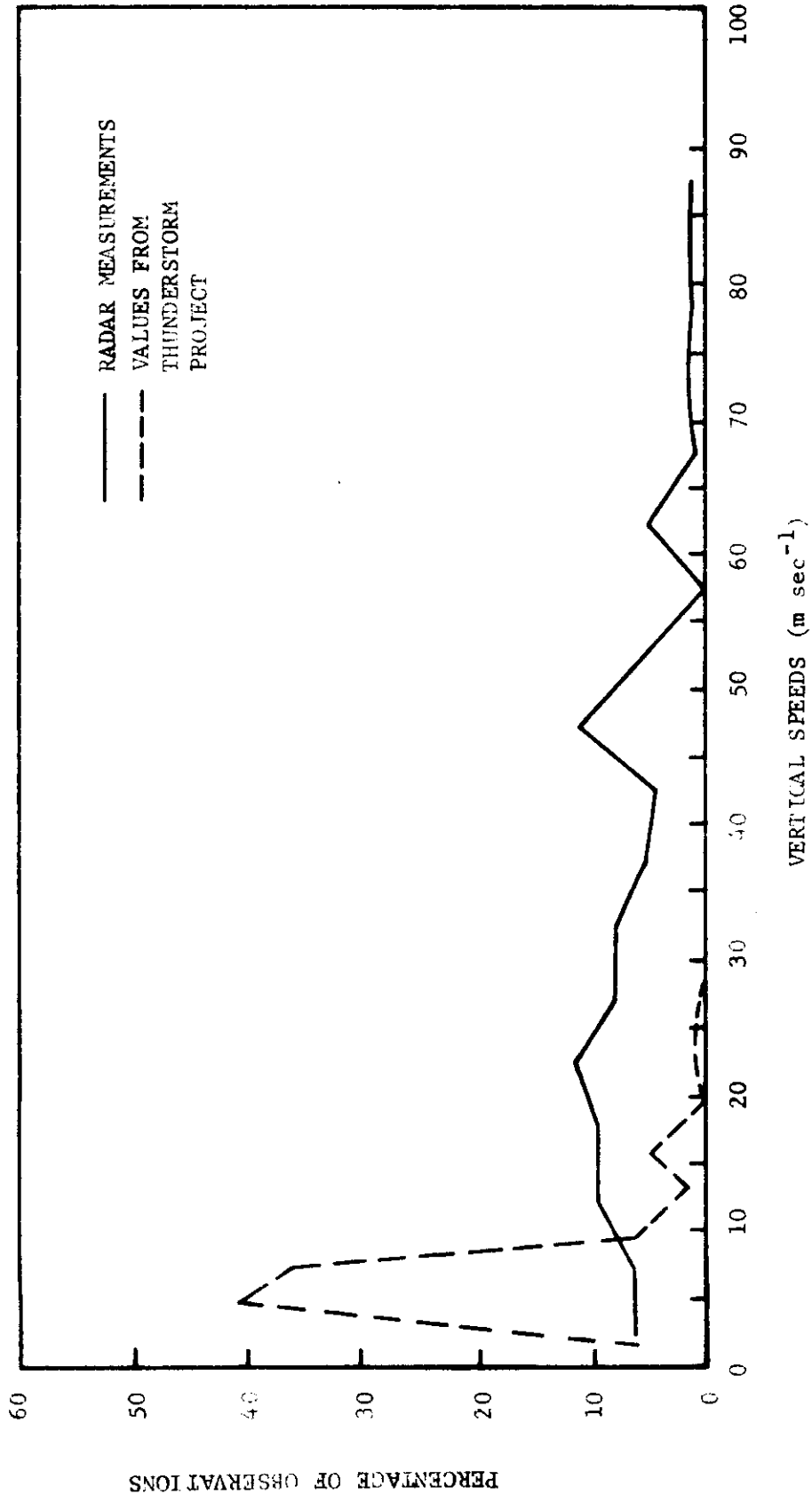


Fig. 8. Percentage of observation of updrafts measured at 11,000 ft.

values in the field to be too large to be accepted. Gradients and time variations of liquid-water content were calculated from the scalar fields. These calculations together with a measure of the rate of growth of rain by coalescence were inserted into a continuity equation which then was solved for point values of vertical speeds. The experimental error was compounded in the computations of the vertical speeds with the result that time-height cross sections of vertical speeds were quite unrealistic. Certain point calculations of vertical speeds were reasonable but many values were extremely large. Groupings of both the measurements of liquid-water content and vertical speeds indicated that the estimated magnitudes of the experimental errors were of the correct order.

## HYDROGRAPH SYNTHESIS

### General

Considerable effort was expended in the development of techniques for synthesis of characteristic hydrographs for any selected drainage basin, gaged or ungaged. Data were utilized in these studies from several small drainage basins in Texas and Oklahoma which are maintained by the Agricultural Research Service (ARS) and the Geological Survey. Particular emphasis was placed on developing methods which would have computer application, also techniques that could be used in possible application to streamflow forecasting.

The results of this study have been summarized by Hudlow (1966, 1967). In particular, a technique for hydrograph synthesis suggested by Snyder (1938) was investigated. Although, the procedure finally developed was considerably modified from that of Snyder, the technique for determination of critical values, e.g., lag, maximum or peak discharge, and hydrograph width, was similar. A modified Pearson type III function was then fit to the critical values so that a continuous hydrograph could be determined. Hudlow and Clark (1969) have presented a detailed discussion of the technique for fitting the Pearson type III function to the selected points.

### Techniques Employed

There are two fundamentally different techniques for hydrograph synthesis. The first of these techniques consists of estimating hydro-

graph parameters, usually peak discharge and some time parameter, from watershed and storm characteristics. From these two parameters and available information concerning the hydrograph shape, the remainder of the hydrograph can be sketched. The second method involves routing of rainfall excess (surface runoff) through catchment storage to produce an outflow hydrograph of surface runoff for a catchment. Both approaches for hydrograph synthesis were utilized in this study.

It is believed that the radar can offer decisive advantages over a sparse rain-gage network when used with either of the foregoing techniques. The radar can supply information concerning the temporal and areal distribution of the rainfall. This information will allow for an accurate evaluation of lag time. Therefore, the capability of the routing procedure to synthesize a complex hydrograph resulting from a non-uniform distribution of rainfall excess was examined.

Hydrograph synthesis with the Pearson type III function. The procedure developed for utilizing the Pearson type III function is illustrated below. The watershed selected was the experimental watershed comprising the drainage area for the Little Washita River in Oklahoma. The watershed is maintained by the Soil and Water Conservation Research Division, ARS, Chickasha, Oklahoma. The Little Washita basin was chosen because of the ample data available from rain-gage, radar, and stream-gage observations. The ARS maintains a dense network of recording rain gages on the Little Washita. The National Severe Storms Laboratory (NSSL), Environmental Science Services (ESSA), Norman, Oklahoma operate a WSR-57 radar which scans the watershed and is within 45 n mi. The WSR-57 radar has a wavelength of 10 cm. Radiation at this wavelength suffers negligible attenuation, even in the heaviest rainfall. From the above, it becomes apparent that this combination of weather radar and instrumented watershed offers excellent opportunities for hydrologic research.

Fig. 9 depicts the Little Washita basin and the ARS rain gage network. Each of these gages is a weighing-type, recording rain gage. The numbers indicate the identifying number assigned to each gage by the ARS. The locations of various Weather Bureau (WB) rain gages, which were used in the analyses, also are shown in Fig. 9.

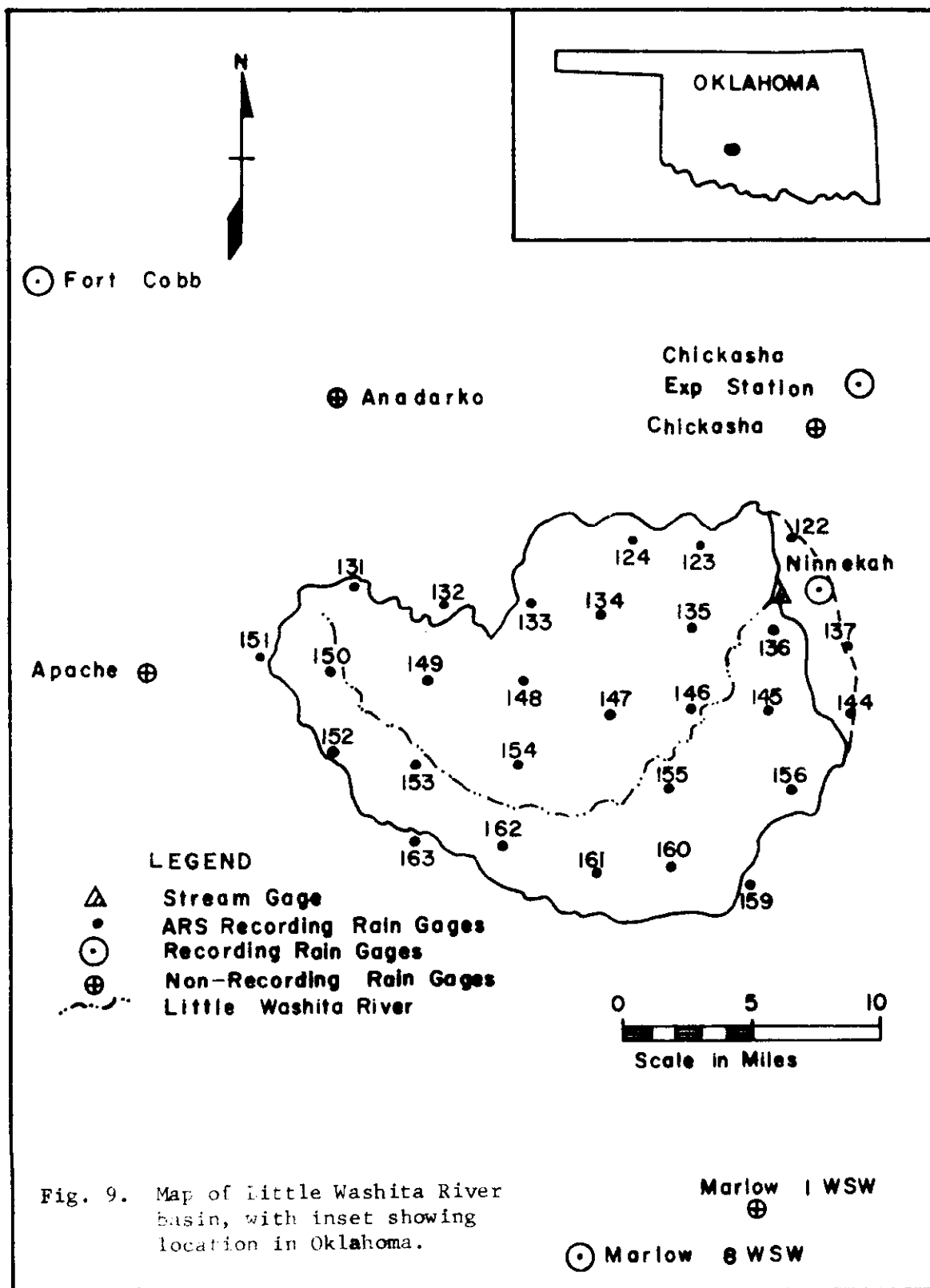


Fig. 9. Map of Little Washita River basin, with inset showing location in Oklahoma.

Marlow 1 WSW  
 ⊕  
 Marlow 8 WSW

The Little Washita River is a tributary of the Washita River, and lies south of the main stream. It flows generally eastward to join the main stream near Ninnekah, Oklahoma. Average discharge for the Little Washita is approximately 40 cfs ( $\text{ft}^3/\text{sec}$ ). The maximum discharge on record of 30,000 cfs, which was estimated from flood marks, occurred in May 1949. Periods of zero flow are observed in some years.

The 210  $\text{mi}^2$  drainage area of the Little Washita River consists of Reddish Prairie and Cross Timber areas. Less than 50 per cent of the area is in cultivation; a large per cent is in open grass land. Principal crops are small grain and cotton.

Although the Little Washita watershed offers excellent opportunities for hydrologic research, a slight drawback exists in its use for a study of this type. Extensive conservation practices are being employed on the watershed. For example, 21 per cent of the drainage area is controlled by farm ponds. ARS hydrologists are studying the effects of man-made conservation measures on streamflow. While such conservation measures act to increase infiltration and reduce erosion, an accompanying reduction in surface runoff will occur. For a "highly conserved basin" the reduction in surface runoff can be appreciable (see Hartman *et al.*, 1967). It was felt that the conservation practices employed on the Little Washita basin acted to reduce the magnitude of the runoff events. For the 7 yr of record (1959-1965) considered for analyses, the largest runoff event selected was 7040 cfs, the next largest was 3800 cfs, and over 70 per cent of the events selected had peak discharges of less than 2000 cfs. The 7040 cfs event represents a discharge of 33 cfs per  $\text{mi}^2$ , while the remainder of the events represent much smaller amounts. Obviously, equations developed from the runoff events described above cannot be used, justifiably, for runoff prediction of large magnitude. However, while the relationships developed for this study were not derived from storms of great magnitude, the techniques presented appear applicable and were used in hydrograph synthesis for this basin and in the study on streamflow forecasting discussed later.

Usually the amount of initial losses, which occur in the early portions of a storm, are a function of the initial soil-moisture conditions. However, in some areas this is not always the case; Schreiber and Kincaid

(1967) found soil moisture to be a parameter that is rarely significant for runoff prediction for an experimental watershed in Arizona. The antecedent precipitation index (API) provides an indicator for initial soil-moisture conditions. Kohler and Linsley (Linsley, Kohler, and Paulhus, 1958, p. 171) propose the equation

$$\text{API} = b_1 D_1 + b_2 D_2 + \dots + b_t D_t \quad (13)$$

where  $b_t$  is a constant less than unity, which decreases exponentially with  $t$ , and  $D_t$  is the amount of daily precipitation which occurs  $t$  days prior to the storm under consideration. The constant  $b_t$ , is given by

$$b = F^t, \quad (14)$$

where  $F$  is a factor less than unity whose value will determine the number of preceding days required in the API determination. The size of  $F$  depends on the soil-cover complex and evapo-transpiration, and therefore will vary somewhat with season. However, the most important factor influencing  $F$  appears to be the soil type (see Minshall, 1960, p. 22). For this reason a fixed value for  $F$ , for a reasonable homogeneous watershed, probably is adequate. A value of 0.85 for  $F$  was adopted for this study. This necessitates an antecedent period of 15 days for the API calculations.

It should be mentioned that other antecedent indicators might be used in association with the radar and operational forecasting. One possibility might be to use an equation analogous to Eq. 13 in which the precipitation amounts are replaced by the number of hours that precipitation is observed during each day. Such an API probably would not provide as good an index of the initial conditions of soil moisture; however, it offers one distinct advantage: it would be simpler to evaluate when utilizing radar data. In the use of weather radar for flood forecasting, it is quite possible that estimates of quantitative precipitation will not be made by radar, unless the storm is sufficiently large to represent a potential flood. However, all rainfall that occurs within a reasonable time span prior to the storm in question, contributes to the initial soil moisture. Although the preceding storms might not appear of sufficient magnitude to warrant a detailed analysis of quantitative precipitation, it



would be a simple matter to keep track of the number of hours that precipitation occurs over sub-regions of the watershed. API as defined by Eqs. 13 and 14 was used exclusively for this study.

Six equations, one for runoff prediction and five for hydrograph synthesis, were developed by the procedure of least squares. All five equations are highly significant statistically.

The equation developed for runoff prediction is the most critical of the six equations. For this reason it will be examined in greater detail than the other five. Runoff prediction is critical because a hydrograph can be determined adequately only if the amount and distribution of the rainfall excess (runoff) is known. This fact will become apparent from later discussions.

Numerous variables may influence the quantity of runoff (rainfall-minus-runoff) resulting from a storm. Storm rainfall, antecedent precipitation, storm duration, rainfall intensity, and time-of-the-year all may have an effect on the amount of runoff accompanying a storm. Various models involving these variables were examined. It became apparent readily that a non-linear equation would be required to predict adequately the runoff. A computer program was written to test the significance of each variable considered in the regression analysis. Storm precipitation was found to play a significant role and no improvement was gained by including storm duration or intensity in the prediction model. The soil-cover complex of the watershed normally changes somewhat with season. For this reason the time of the year was considered as a possible factor for inclusion in the prediction equation for runoff. However, for the 18 storms considered in this study there was no enhancement in the regression model due to time of the year.

The equation selected for runoff prediction includes storm precipitation and an index of initial soil-moisture (API). The "Cobb-Douglas" function was selected as the most appropriate model. The equation obtained is

$$E = 0.0961 \bar{R}^{-0.81} \text{API}^{0.357}, \quad (15)$$

where  $\bar{R}$  is the average rainfall for the storm in inches; API is the antecedent precipitation index, in inches; and E is the rainfall excess (runoff)

in inches. For the least-squares procedure the "Cobb-Douglas" function was linearized by a logarithmic transformation. Sharp *et al.* (1960) have pointed out that for many hydrologic variables (e. g., runoff) the assumption that the variance of the dependent variable does not depend on the values of the independent variables is not wholly justified. Therefore, a logarithmic transformation, which necessitates a multiplicity error-term, should make the use of multiple-regression analysis satisfactory for such hydrologic investigations.

One possible improvement in Eq. 15 might have been achieved by considering antecedent precipitation longer than 15 days for the API calculations. Nonetheless, Eq. 15 satisfactorily predicted the runoff events of small magnitude for the case studies while it appreciably under-estimated the one event of large magnitude used in the case studies.

The peak discharge of a hydrograph is a function of the areal distribution of the rainfall excess as well as the amount of runoff. As illustrated by the Soil Conservation Service (1957, p. 3.15-1) lag time may be thought of as an average travel time for the watershed.<sup>1</sup>

$$Lg = \sum_{i=1}^W \frac{(a_i e_i t_{ci})}{A_t E} , \quad (16)$$

where  $a_i$  is the area of the  $i^{\text{th}}$  subarea (see Fig. 10);<sup>2</sup>  $e_i$  is the rainfall excess for the  $i^{\text{th}}$  subarea;  $t_{ci}$  is the mean travel-time for the  $i^{\text{th}}$  subarea;  $A_t$  is the area for the portion of the watershed that experiences rainfall excess;  $E$  is the total runoff for the watershed; and  $W$  is the total number of subareas.

From the definition, Eq. 16, it is apparent that the lag time is a function of the areal distribution of the rainfall excess. Therefore lag time and total runoff were used as the independent variables for the prediction of peak discharge. Once again, the "Cobb-Douglas" function was selected as the appropriate model. The resulting equation is .

$$Q_p = 58460 E^{0.944} / Lg^{0.642} , \quad (17)$$

---

<sup>1</sup>Time of concentration is the time required for water to travel from the hydraulically most distant portion of an area or rainfall excess to the watershed outlet.

<sup>2</sup>For this study the watershed is divided into subareas bounded by the isochrones needed for evaluating Eq. 16 (see Fig. 10).

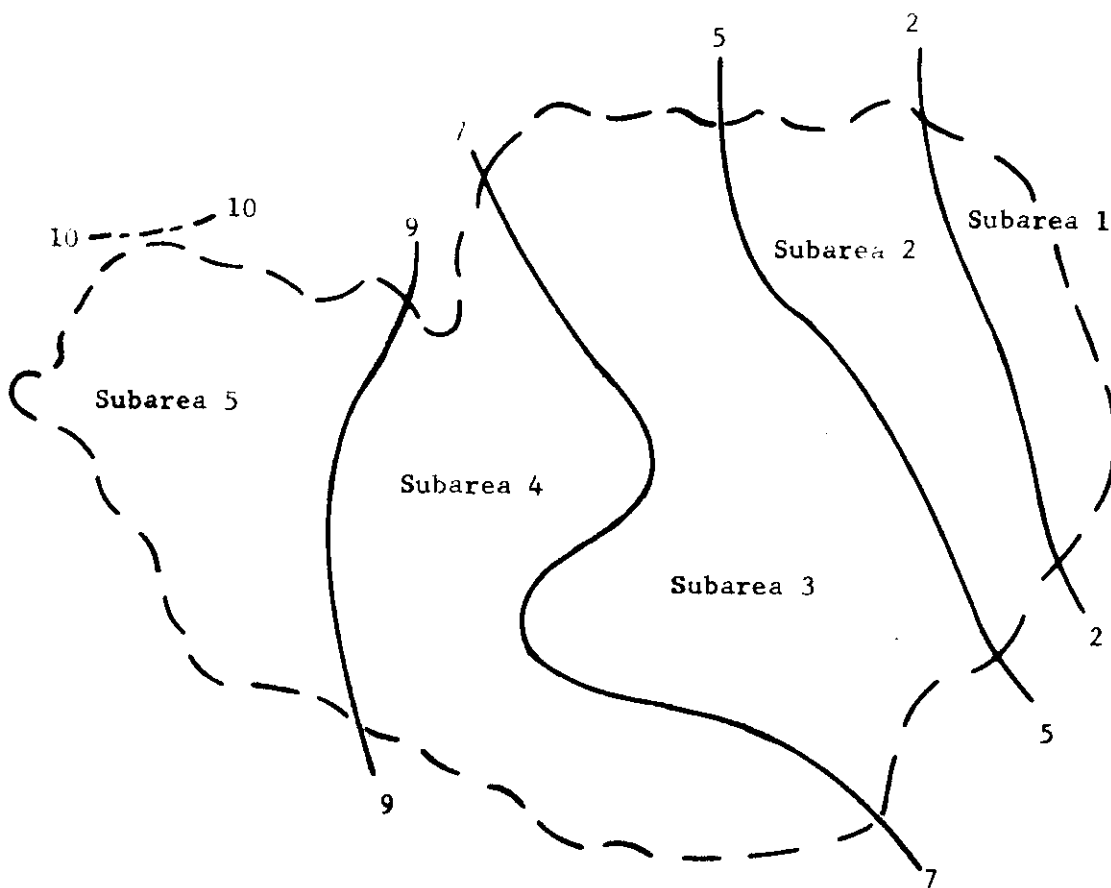


Fig. 10. Isochrones for the Little Washita (hr).

where  $Q_p$  is the peak discharge of the hydrograph in cfs;  $E$  is in inches; and  $Lg$  is in hours.

In order to establish the hydrograph period of rise, a relationship was sought between  $T_p$  and  $Lg$ , where  $T_p$  is equal to the period of rise of the hydrograph minus the time elapsed between the beginning and the centroid of the rainfall excess. For any one watershed the ratio of  $T_p$  to  $Lg$  should be essentially constant because the hydraulic characteristics of most basins change inappreciably. Therefore, a linear relationship was assumed and a regression equation obtained by "least squares" for the  $T_p$  versus  $Lg$  data. Initially, the line was not required to pass through the origin; however, the null hypothesis that the intercept equals zero was accepted. Next, a straight line passing through the origin was derived. The resulting equation is

$$T_p = 0.823 Lg , \quad (18)$$

where both  $T_p$  and  $Lg$  are in hours.

In order to describe the complete hydrograph by the technique described in the following section, expressions for the width of the hydrograph at 50 and 75 per cent of the peak discharge must be derived. Since the shape of simple hydrographs for a given basin remain reasonably unchanging, a relationship should exist between the width of the hydrograph, at a fixed per cent of the peak discharge, and the period of rise. The hydrograph width should increase from a very small value, for an extremely short period of rise, to larger values, for longer periods of rise.

A plot on semi-logarithmic paper of the hydrograph width at 50 per cent of the peak discharge versus the period of rise revealed the relationship as exponential. The least-squares solution gave

$$W_{50} = 2.25 \exp[0.107 P_r] , \quad (19)$$

where  $W_{50}$  is the width of the hydrograph at 50 per cent of the peak discharge in hours, and  $P_r$  is the hydrograph period of rise in hours.

For the same watershed a relationship must exist between  $W_{75}$  (hydrograph width at 75 per cent of the peak discharge) and  $W_{50}$ . A direct relationship between  $W_{75}$  and  $W_{50}$  assures that the shape of the hydrograph conforms to the characteristic shape for the watershed. A straight-line relationship with zero intercept was chosen as the

appropriate model. The least-squares solution gave

$$W_{75} = 0.558 W_{50} , \quad (20)$$

where both  $W_{75}$  and  $W_{50}$  are in hours.

From Eqs. 15, 16, 17, 18, 19, and 20 and two additional relationships concerning the positioning of the hydrograph widths at 0, 50, and 75 per cent of the peak discharge, seven points on the hydrograph may be determined. The Corps of Engineers have suggested, as a guide for shaping the hydrograph, that the hydrograph widths at 50 and 75 per cent of the peak discharge should be positioned so that one-third of the width is placed to the left and two-thirds of the width to the right of the hydrograph peak. However, this research has indicated that an allocation of four-tenths of the width to the left and six-tenths of the width to the right produces optimum results.

One other relationship is needed, this being a relationship for the base width of the unit hydrograph. Following the practice of the Soil Conservation Service and the Corps of Engineers, a base width of  $5 P_r$  was adopted.

The Pearson type III function was selected as the most appropriate mathematical function for fitting the seven points. This function can be written as

$$Q = Q_p (T/P_r)^a \exp[-(T-P_r)/c] , \quad (21)$$

where  $Q$  is the discharge in cfs at any time  $T$ ;  $T$  is the time in hours from the beginning of rainfall excess;  $Q_p$  is the peak discharge in cfs;  $P_r$  is period of rise of the hydrograph in hours;  $a$  is a dimensionless constant for a particular hydrograph; and  $c$  is a constant for a particular hydrograph, expressed in units of hours. Two iterative procedures are combined to solve for the  $c$  and  $a$  that give a least-squares fit of Eq. 21 to the seven points.

Hydrograph synthesis by runoff routing. From an intensive study of routing procedures, Laurenson (1962) has concluded that a general procedure for runoff routing should provide for:

1. Temporal variations in rainfall excess.
2. Areal variations in rainfall excess.
3. Different elements of rainfall excess passing through different amounts of storage.

4. Catchment storage being distributed rather than concentrated.
5. A non-linear relationship between stream discharge and catchment storage.

Based on the study of 1962, Laurenson (1964) published a description of a procedure for runoff routing which provides for these five occurrences. His work was used as a guide for deriving the runoff-routing model adopted for this study. However, the procedure used in the derivation of the routing model differs in two respects from that of Laurenson:

1. Time of concentration, instead of lag time, was selected as the time parameter used in the isochrone construction. All travel times were considered a fraction of the time of concentration.
2. Identification of a possible non-linear relationship between stream discharge and catchment storage was accomplished from examination of concentration times, instead of lag times, for selected storms.

Laurenson implies that the relationship between stream discharge and catchment storage is generally nonlinear. This means that the storage-delay time, for a given subarea, varies with the magnitude of the outflow from the subarea. If we assume that only prism storage exists (see Linsley, Kohler, and Paulhus, 1958, p. 227), the storage-discharge relationship may be expressed as

$$S_i = K_{si} (O_i) O_i , \quad (22)$$

where  $S_i$  is the storage for the  $i^{\text{th}}$  subarea for a given outflow and  $K_{si}$  is the storage coefficient (storage delay time) for the  $i^{\text{th}}$  subarea;  $(O_i)$  indicates that the storage coefficient may be a function of the outflow.

The subareas used for the routing procedure are the same as those used for hydrograph synthesis with the Pearson type III function. The isochrones were constructed based on the assumption that travel time is proportional to

$$L/\sqrt{S} , \quad (23)$$

where  $L$  is the length of the flow path and  $S$  is the slope of the flow path. Such a relationship can be supported by the Chezy formula (see Chow, 1964, p. 7-23). The following steps were taken in the construction of the isochrones.

1. An average time of concentration was determined from hydro-graph analysis of selected storms (see Johnstone and Cross, 1949, p. 229).
2. A large number of points were located on a topographic map of the watershed.
3. Travel times for each point were obtained from two applications of Eq. 23. The total travel time was assumed equal to the sum of the travel times for overland flow and channel flow.

The isochrones are those shown in Fig. 10.

The fundamental equation used for runoff routing (mass continuity equation) can be expressed as

$$(I_1 + I_2) \frac{\Delta t}{2} - (O_1 + O_2) \frac{\Delta t}{2} = S_2 - S_1, \quad (24)$$

where  $I$  is inflow,  $O$  is outflow, here  $S$  refers to storage, and the subscripts 1 and 2 refer to the beginning and end of the routing period ( $\Delta t$ ), respectively. Substitution for  $S_2$  and  $S_1$  from Eq. 24 yields

$$O_2 = C_0 I_2 + C_1 I_1 + C_2 O_1, \quad (25)$$

where

$$C_0 = C_1 = \Delta t / (2K_{s2} + \Delta t)$$

and

$$C_2 = (2K_{s1} - \Delta t) / (2K_{s2} + \Delta t). \quad (26)$$

Since  $C_0$ ,  $C_1$ , and  $C_2$  depend on  $K_{s2}$ , an iterative solution of the system of routing equations is required if  $K_{s2}$  is a function of  $O_2$  (non-linear model).

Laurenson assumed that there exists a non-linear relationship between stream discharges and catchment storage if the lag time varies significantly with average discharge for selected storms. However, an examination of the variability of  $T_c$  with  $Q_p$  appears to represent a more logical approach. This is because lag time is highly dependent

on the distribution of the rainfall excess. For watersheds with areas larger than a few square miles, it becomes difficult to find storms that are evenly distributed over the basin. Nevertheless, the distribution of the rainfall excess is not a critical factor in the evaluation of the time of concentration.

Eight storms over the Little Washita were selected for an examination of  $T_c$  (time of concentration). On a plot of  $T_c$  versus  $Q_p$  there was no indication that a significant relationship existed solely between  $T_c$  and  $Q_p$ . Therefore, a linear routing model was adopted. Since the model was assumed to be linear, the principle of superposition is applicable. Rainfall excess from each subarea was routed independently to the outlet, and the five separate outflows were combined.

Table 2 gives the storage coefficients for the five subareas used with the routing model.

Table 2. Storage coefficients for the Little Washita

Subarea	1	2	3	4	5
$K_{si}$ (hr)	1.0	3.5	6.0	8.0	9.5

#### An Example

A hydrograph was synthesized for the storm of May 9, 1965, based on the rainfall measurements from the ARS network using the Pearson type III function. Also, since this storm was complex (two peaks), it was selected as the "test storm" for the routing model. The hydrographs synthesized for that storm are presented in Fig. 11. It was hoped that the routing model would satisfactorily reproduce the two peaks observed for that storm but it failed to do so. The two peaks were not the result of two separate bursts of rainfall but, rather, are a result of an uneven distribution of rainfall excess which occurred over the basin. The tributary arrangement in the vicinity of the maximum rainfall gave a large gradient of travel time. This fact, coupled with the large gradients of precipitation in this same locality, is believed to be responsible for the occurrence of the two peaks. However, for the combination of subareas selected (see Fig. 10), the



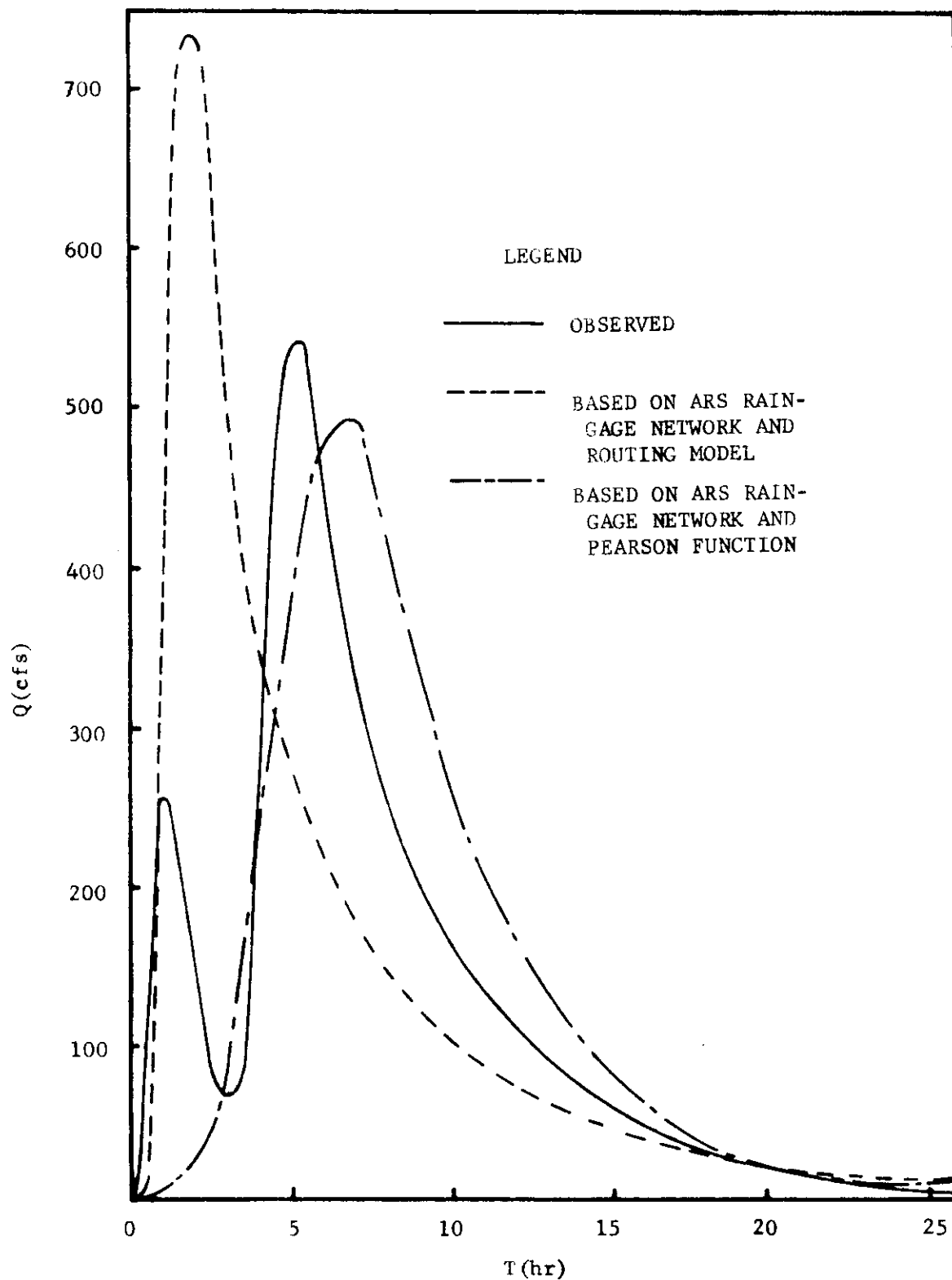


Fig. 11. Comparison of synthesized hydrographs to the observed hydrograph for the storm of May 9, 1965. Little Washita River nr. Ninnekah, Oklahoma.

routing procedure was unable to detect the two peaks. In fact, it actually predicted the hydrograph peaks several hours earlier than the Pearson function.

A possible improvement in the routing procedure might be attained by considering a series of linear storages between each subarea and the outlet. That is, the total storage delay time for each subarea could be segmented into several storage coefficients and multiple routing performed from each subarea to the outlet. Laurenson (1962, Sect. 5.5.1) has investigated a linear routing model which assumes a series of concentrated storages between each subarea and the outlet. Laurenson concluded that a non-linear routing model was more appropriate for his basin. However, since the storage equation for the Little Washita is assumed to be linear, a procedure similar to the one investigated by Laurenson for linear routing might represent an improvement over the routing model adopted for this study.

## STREAMFLOW FORECASTING

### General

Data were not available immediately from the radar system in the Department of Meteorology, Texas A&M University, in the early stages of this project. Therefore the data obtained from NSSL and the Experimental Watershed in the Washita River basin maintained by the ARS near Chickasha, Oklahoma, were used. Since both areal and temporal variation of rainfall is important in streamflow forecasting, accurate and rapid hydrograph synthesis, as discussed above, is of equal importance. The utilization of radar data in streamflow forecasting was emphasized in this study.

### Success of Runoff Predictions

Table 3 summarizes the runoff based on the various rainfall measurements. For determination of rainfall utilizing radar data Eq. 2 was used in which  $A = 200$  and  $B = 1.6$ . The predictions may be compared to each other and to the observed runoff, which also is listed in Table 3. The following observations can be made from Table 3.

Table 3. Average precipitation and runoff derived from various rainfall measurements compared to each other and to observed runoff.

Storm No.	Date	ARS Rain-Gage Network		NSSL Radar		Two Rain Gages (ARS Gages 137 and 151)		Observed	
		P(in)	E(in)	P(in)	E(IN)	P(in)	E(in)	P(in)	E(in)
19	5/9/64	2.10	0.166	0.85	0.075	1.83	0.137	-----	0.385
20	5/9/65	0.49	0.025	0.28	0.017	0.61	0.027	-----	0.024
21	5/30/64	0.26	0.041	0.60	0.080	0.14	0.022	-----	0.031
22	5/10/64	0.59	0.079	0.47	0.067	0.86	0.106	-----	0.086

1. Runoff was forecast from measurements by radar for all four storms.
2. For the four storms the runoff predictions derived from the two ARS rain gages are as good as or better than the predictions from radar measurements.
3. Appreciable error was made in the runoff prediction for storm 19 even with measurements taken with the dense ARS rain-gage network.

Based on observation No. 1 it might be concluded that the radar possesses potential for use as a hydrologic tool. The prediction of an amount of runoff, even though the prediction may be in error, is better than no prediction. This result indicates that if no rain gages are available, the radar, even under the worst circumstances, will yield answers that are better than no answers.

The two ARS rain gages constitute a gage density which is superior to that normally encountered for hydrologic work. In addition, the location of the two gages on opposite ends of the watershed constitute an optimum gage arrangement. While the quantitative prediction of precipitation and runoff derived from measurements taken with the two ARS gages appear somewhat superior to those based on radar measurements, the radar actually proved superior for depicting the spatial distribution of the rainfall for storm 20.

Observation No. 3 stresses the importance of obtaining a satisfactory equation for runoff prediction, Eq. 15. The inadequacies accompanying the derivation of Eq. 15 were discussed. Great effort should be placed on the development of the equation for prediction of runoff for operational forecasting. The equation, hopefully, should lead to forecasts of accurate amounts of runoff for a storm of any magnitude.

#### Comparison of Lag-Time Estimates

Table 4 lists the estimates of lag time as derived from various rainfall measurements. Also, the observed lag times are presented for comparison. The estimates of lag time, based on measurements performed with radar, are excellent for both storms 19 and 20; the differences between the predicted and observed lag times were less than 3 per cent

Table 4. Lag times and peak discharges derived from various rainfall measurements compared to the observed values.

Storm No.	Date	ARS Rain-Gage Network		NSSL	Radar	Two Rain Gages (ARS Gages 137 and 151)		Observed	
		Lg (hr)	$Q_p$ (cfs)			Lg (hr)	$Q_p$ (cfs)		Lg (hr)
19	5/9/64	6.43	3250	6.73	1495	6.98	2570	6.85	9190
20	5/9/65	7.30	500	6.55	367	8.10	503	6.75	540

in both instances. The estimate of the lag time for storm 19, derived from rainfall measurements taken with the two ARS rain gages, also is very good. Storm 19 was evenly distributed over the watershed. Therefore, a lag-time estimate based on only two rain gages gave satisfactory results. However, appreciable error (20 per cent) occurred in the estimate for lag time, derived from the two rain gages, for storm 20. This sizable error emphasizes the superiority of the radar over a sparse rain-gage network for depicting the spatial distribution of rainfall when a storm is unevenly distributed over the basin.

#### Stochastic Model for Rainfall-Runoff Simulation

Rainfall model. In recent years the term stochastic hydrology has received widespread usage. Stochastic hydrology is defined as the manipulation of statistical characteristics of hydrologic variables to solve hydrologic problems. One such stochastic technique involves the use of a Markov chain for the simulation of rainfall and/or runoff. A. A. Markov (1856-1922), a Russian probabilist, introduced the concept of a stochastic process known as the Markov process, or Markov chain (see Parzen, 1960). In the classical sense, for a Markov process, the probability of a system experiencing a given state depends only on the knowledge of the state of the system at the immediately preceding time. However, in recent years it has become customary to consider stochastic processes with greater than first-order time dependencies as Markov chains. For example, if the existing state depends on the two immediately preceding times and corresponding states, such a process is called a second-order Markov chain. Nth order chains are defined similarly. If the existing state depends only on the immediately preceding time and state, such a process is called a first-order Markov chain or simply a Markov chain. A first-order Markov chain can be said to exist if the

$$P(X_{t+1} | X_t, X_{t-1}, \dots, X_1) = P(X_{t+1} | X_t), \quad (27)$$

where P denotes the probability of occurrence of the quantity within parentheses,  $X_t$  denotes the amount at time t, and the slash can be read as "given that." The set of probabilities for all states in the system forms what is called the matrix of transitional probabilities.

The transitional probabilities define the chain (see Parzen, 1960). If the transitional probabilities are considered time independent, the Markov chain is called homogenous or stationary. Once the transitional probabilities have been established, the discrete distribution can be synthesized by Monte Carlo (random) selection of the probabilities and corresponding amounts.

In order to justify the use of a Markov chain for depiction of the hourly rainfall process (hourly amounts are considered for this study), we must first establish that hourly precipitation is a non-random occurrence. Serial correlation coefficients are indicators of the non-randomness of a time series. Serial correlation coefficients for hourly rainfall were computed and correlograms were plotted for 100 storms occurring at Ninnekah, Oklahoma. A correlogram is a graphical representation of  $r_k$  versus  $k$  (lag), where  $r_k$  is the  $k^{\text{th}}$ -order serial correlation coefficient. For the storms of sufficient duration to warrant significance tests for  $k = 1$  ( $N > 7$ ),  $r_1$  was almost always significantly different from zero. Generally for  $k \geq 2$ ,  $r_k$  was found insignificant. The average correlogram, as computed from the ten longest storms ( $N \geq 20$ ), is shown in Fig. 12. Since  $r_1$  is significantly different from zero, it can be concluded that the hourly rainfall process is a non-random occurrence for which the present state depends on the immediately preceding period. Fig. 12 shows  $r_k$  decreasing monotonically with increasing  $k$  and thus supports the autoregressive or Markov process.

Pattison (1965) has used a Markov-chain model for synthesizing hourly amounts of rainfall. Pattison's model was designed for use with the Stanford Watershed model (Crawford and Linsley, 1962); it has produced satisfactory results at several locations in California. Pattison (1964) observed some important features of the rainfall process; two of these are worth noting:

1. Most rainfall systems produce sporadic rain.
2. The rainfall-producing process which exists at any given time is in a state which was achieved by the interaction of the conditions which existed during the immediately preceding period.

It is interesting to note that feature 2 is in exact agreement with re-

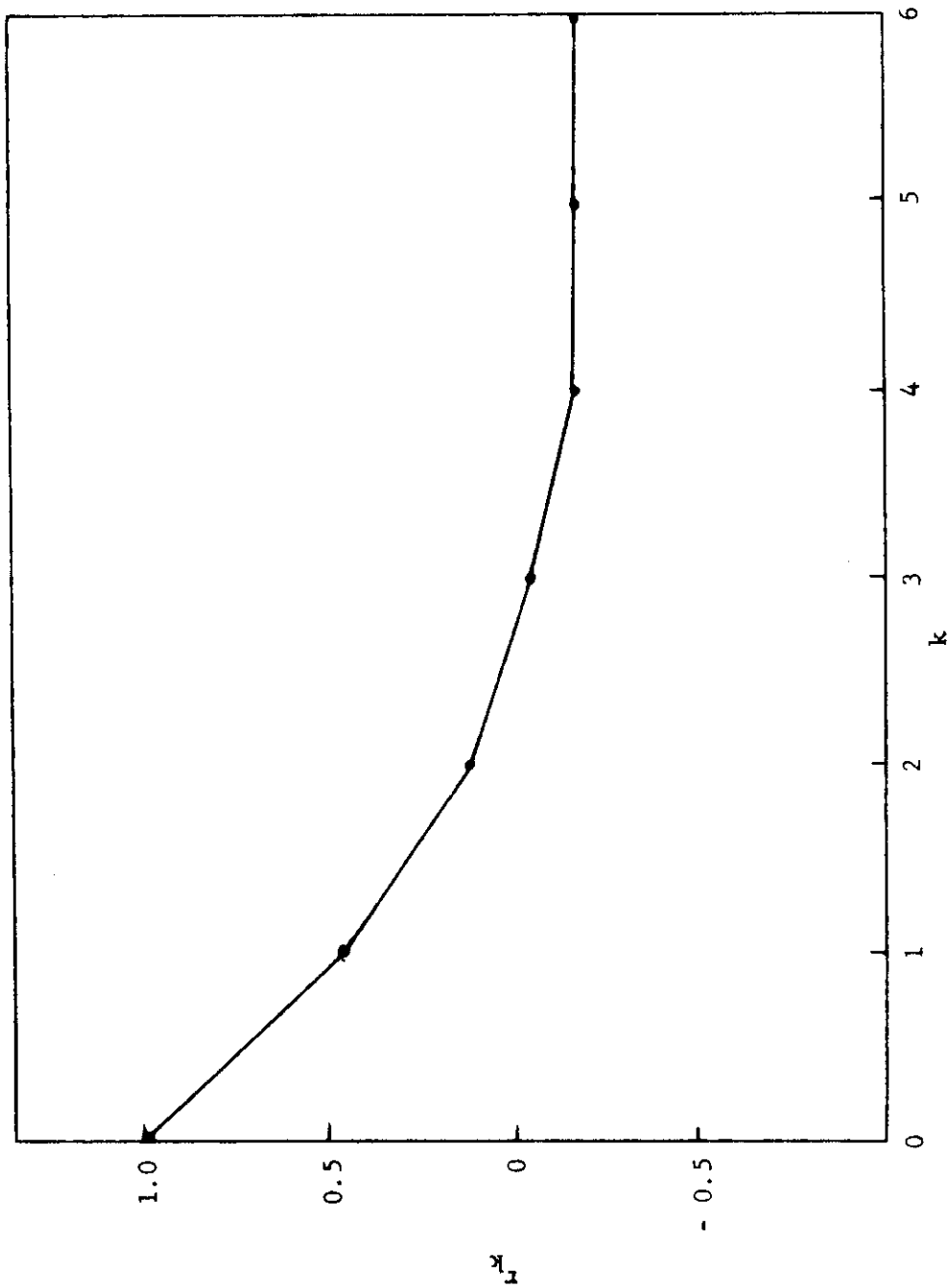


Fig. 12. Average correlogram of hourly rainfall at Ninnekah, Oklahoma.



sults obtained from the serial correlation analysis above.

Pattison's model (1965) provided for inclusion of the dry hours which occur during sporadic rain storms. Pattison assumed the transition probabilities to be stationary within each month of the year but to vary from month to month. The Markov chain developed for this study differs basically in three respects from Pattison's:

1. Synoptic type replaces the month of the year for the stationary periods.
2. Diurnal persistence is considered during dry hours.
3. The model was derived for a different area.

Huddle (1967) has proposed a Markov-chain model and presented the transitional probabilities for the hourly rainfall process at Ninnekah, Oklahoma. The chain was derived from approximately 175 scattered months of hourly precipitation data from the periods 1940-1942 and 1949-1966. Huddle's work was initiated partially for the purpose of furnishing this study with a satisfactory rainfall model. The model is used, as described below, to provide the precipitation input for runoff synthesis.

As illustrated above, the basic-synthesis procedure should involve the autoregressive or Markov process. Pattison (1964) has investigated the possibility of using a linear autoregression model for the first order. In this study the Markov chain has proved superior to the linear model. A non-linear autoregressive model might prove successful; however, a Markov chain coupled with Monte Carlo simulation offers greater flexibility.

The Markov chain proposed by Huddle, like Pattison's, consists of a primary and a secondary portion. The primary considers only first-order dependencies and is used exclusively during sequences on non-zero rainfall (wet hours). However, as soon as a dry hour is forecast the secondary portion of the chain, which considers sixth-order dependencies, must be adopted. The over-all simulation procedure involves an interplay between the primary and the secondary portions of the chain.

Because of the relatively short period of record available at Ninnekah, a restricted number of rainfall classes was considered. If too many classes were used, meaningful probabilities could not be

assessed. In addition, the greater the number of classes, the greater the computational difficulties. A practical number had to be adopted which was compatible with the purpose of the model. Huddle selected ten classes for the hourly amounts of rainfall (see Table 5). The hourly process is recovered in the simulation scheme by selecting the mean rainfall for the class. The mean rainfalls for the classes, as determined from the 175 months of useful record, also are presented in Table 5.

Since the synoptic situations which can produce rainfall in Oklahoma differ in type, it was decided that the stationary periods adopted for this study would consist of six synoptic types. As indicated by Huddle, the synoptic situation which occurs is somewhat related to the time of the year, i.e., the two are not independent. It is likely that utilization of both variables would yield improved results. This was not possible for this study because only 15 yr of data were available. Any further division of the data into separate groups would have resulted in frequencies so low as to make it impossible to calculate meaningful probabilities.

Hiser (1956) has separated the precipitation observed in Illinois into six synoptic types. Hiser's classifications are: (1) cold front; (2) warm front; (3) stationary front; (4) squall line; (5) warm air mass; and (6) cold air mass. Consideration of synoptic situations which produce precipitation in Oklahoma led to the conclusion that these six types constitute a valid scheme of classification.

Huddle assigned each day of rainfall, throughout the 175 months of acceptable record at Ninnekah, Oklahoma, to one of the above synoptic types. The procedure admittedly was somewhat subjective, but, as stated by Huddle, in perhaps one-half of the cases a decision could be made with very little doubt of accuracy. The summer months contributed a large number of clear-cut occurrences of type 5 (warm air mass) rainfall, while the winter months logically contributed a large number of type 1 (cold front) occurrences. Decisions were difficult for the cases where a front was more or less stationary in the area. In such cases, type 3 was sometimes appropriate, although types 1, 2, and 5 also had to be considered.

Table 5. Classes of hourly amounts of rainfall and mean rainfall for the classes

Class	Amount	Mean Amount for Class
1	0.00	0.00
2	0.01	0.01
3	0.02-0.03	0.024
4	0.04-0.06	0.048
5	0.07-0.10	0.087
6	0.11-0.20	0.150
7	0.21-0.30	0.254
8	0.31-0.40	0.352
9	0.41-0.70	0.542
10	>0.70	1.000

An example of the first-order transitional probabilities is presented in Table 6. These are the probabilities for synoptic type 3 (stationary front).

An acceptable rainfall model must be capable of reproducing, for sporadic rain, the dry hours dispersed among the wet ones. For this purpose a secondary portion of the Markov chain was developed. The decision of whether an additional dry hour or hours should be forecast, following a dry hour prediction from the first-order transitional probabilities, involves a longer time dependency than first-order. Pattison (1965) considered a sixth-order dependency. In an attempt to determine the time dependence necessary for Oklahoma, Fig. 13 was constructed. This figure illustrates the P (wet hour|number of preceding dry hours). These results are based on Huddle's 175 months of rainfall record. Fig. 13 shows the probability of a wet hour decreasing monotonically to essentially zero for five preceding dry hours.

The primary portion of the Markov chain consists of ten possible states for time (t). These ten states correspond to the ten classes discussed above. Time (t-1) is assigned to one of the ten states, the state depending on the amount of precipitation observed. It might be desirable to retain this much information about each preceding hour, but the number of possible sequences become prohibitively large. Thus, it is necessary to limit the length of sequences or to reduce the number of possible states allowed. As described above, at least a fifth-order dependency should be used for the secondary portion of the Markov chain. Therefore, instead of the ten states used for time (t-1), only two states, wet and dry, were used for times (t-2), (t-3), (t-4), and (t-5).

In order to allow for daily persistence, time (t-6) was defined to comprise a 24-hr period, whereas all periods from time (t) through time (t-5) are equal to 1 hr. Time (t-6) ends with the hour immediately preceding time (t-5). Table 7 gives the transitional probabilities for the secondary portion of the Markov chain. D and W denote dry and wet, respectively. The secondary portion is assumed stationary for all time periods. Table 8 illustrates the complete scheme (primary and secondary portions) for the sixth-order Markov chain.

Table 6. First-order transitional probabilities for synoptic type 3  
(stationary front)

	State During Hour (t)									
	1	2	3	4	5	6	7	8	9	10
1	-----	0.247	0.209	0.138	0.130	0.117	0.054	0.013	0.050	0.042
2	0.490	0.245	0.132	0.063	0.025	0.020	0.013	0.006	0.006	0.000
3	0.404	0.192	0.199	0.089	0.021	0.055	0.020	0.020	0.000	0.000
4	0.318	0.150	0.121	0.050	0.112	0.103	0.028	0.009	0.009	0.000
5	0.295	0.032	0.147	0.158	0.168	0.137	0.042	0.021	0.000	0.000
6	0.228	0.026	0.096	0.123	0.150	0.219	0.079	0.035	0.009	0.035
7	0.089	0.054	0.054	0.018	0.179	0.232	0.179	0.036	0.071	0.088
8	0.071	0.071	0.107	0.143	0.036	0.143	0.250	0.107	0.036	0.036
9	0.200	0.080	0.080	0.120	0.040	0.040	0.160	0.160	0.000	0.120
10	0.037	0.037	0.037	0.074	0.037	0.333	0.074	0.185	0.075	0.111

State During Hour (t-1)

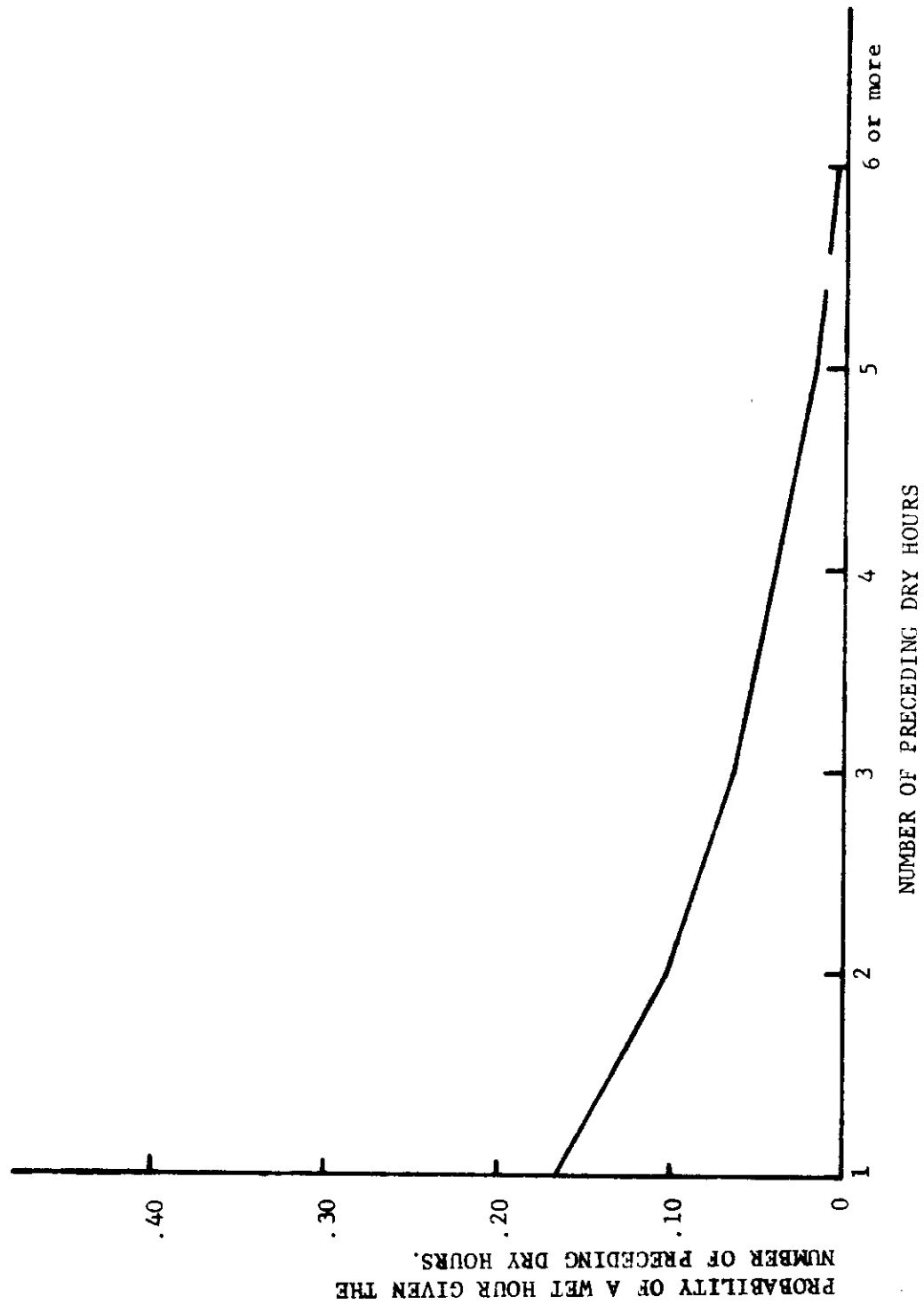


Fig. 13. Transition probabilities following dry periods.

Table 7. Transitional probabilities for the secondary portion of the Markov chain

State During Time						State During Time (t)	
t-6	t-5	t-4	t-3	t-2	t-1	D	W
D	D	D	D	D	D	.995	.005
D	D	D	D	W	D	.943	.157
D	D	D	W	D	D	.915	.085
D	D	D	W	W	D	.789	.211
D	D	W	D	D	D	.947	.053
D	D	W	D	W	D	.556	.444
D	D	W	W	D	D	.937	.063
D	D	W	W	W	D	.857	.143
D	W	D	D	D	D	.968	.032
D	W	D	D	W	D	.667	.333
D	W	D	W	D	D	.800	.200
D	W	D	W	W	D	.875	.125
D	W	W	D	D	D	.924	.076
D	W	W	D	W	D	.714	.286
D	W	W	W	D	D	.927	.073
D	W	W	W	W	D	.866	.134
W	D	D	D	D	D	.984	.016
W	D	D	D	W	D	.830	.170
W	D	D	W	D	D	.865	.135
W	D	D	W	W	D	.783	.217
W	D	W	D	D	D	.933	.067
W	D	W	D	W	D	.783	.217
W	D	W	W	D	D	.866	.134
W	D	W	W	W	D	.878	.122
W	W	D	D	D	D	.960	.040
W	W	D	D	W	D	.781	.219
W	W	D	W	D	D	.887	.113
W	W	D	W	W	D	.814	.186
W	W	W	D	D	D	.938	.062
W	W	W	D	W	D	.723	.277
W	W	W	W	D	D	.897	.103
W	W	W	W	W	D	.834	.166

Table 8. Complete scheme for the sixth-order Markov chain

Time Period Used in Model	Clock Hour	Possible States
Time (t)	Hour (t)	Class 1, 2, ..., 10
Time (t-1)	Hour (t-1)	Class 1, 2, ..., 10
Time (t-2)	Hour (t-2)	Wet - or - Dry
Time (t-3)	Hour (t-3)	Wet - or - Dry
Time (t-4)	Hour (t-4)	Wet - or - Dry
Time (t-5)	Hour (t-5)	Wet - or - Dry
	Hour (t-6)	
	Hour (t-7)	
Time (t-6)	.	Wet - or - Dry
	.	
	Hour (t-29)	



Rainfall-runoff simulation. Monte Carlo simulation with the Markov chain is basically simple. Regardless of whether the primary or the secondary portion of the chain is being employed, the fundamental procedure is as follows:

1. Obtain the cumulative probabilities corresponding to the existing rainfall type and state. The final cumulative probability should be unity.
2. A number from zero to unity is drawn from a sequence of random numbers which are uniformly distributed.
3. The state for time (t) is selected to correspond to the smallest cumulative probability greater than the random number.

The aim of the present study was to use the Markov-chain model presented above as a forecast tool for an individual storm. Knowing the amount of rainfall that occurred during time (t-1) and the preceding 28 hr period, one can make a probabilistic forecast for the next hour, time (t). Time (t) then becomes time (t-1), time (t-1) becomes time (t-2), etc., and the procedure is iterated. Six-hour precipitation forecasts are used in this study.

Six-hour precipitation forecasts were made for each subarea of the watershed (see Fig. 10). The 29 hr of antecedent rainfall needed for the Markov chain simulation was assumed to be the average rainfall for the subarea, and the rainfall forecast for each subarea was assumed to be the average for the subarea. To test the procedure, forecasts were made for two events in which data could be obtained from the ARS rain-gage network (see Fig. 9). Once the forecast rainfall for each subarea was determined, the runoff for each subarea was calculated by Eq. 15. After the runoff for each subarea was obtained, the lag time and peak discharge then could be computed from Eqs. 16 and 17, respectively. The computed peak discharge then was deposited in one of one hundred equally-spaced classes. The classes were divided into 100-cfs class intervals and, thus, encompass discharges from 0 to 10,000 cfs. The simulation procedure was repeated for a total of 500 iterations. The forecast procedure would be the same regardless of the source of rainfall information, e.g., radar-estimated rainfall.

A Fortran IV computer program was written for the rainfall-runoff simulation. The computer output consisted of a frequency histogram of hydrograph-peak discharges and corresponding lag times. From the frequency histogram, the peak discharge and lag time occurring with the greatest frequency was determined; this peak discharge then represented the most probable value. Similarly, peak discharges of various frequencies and corresponding probabilities were obtained.

The forecasts of rainfall and runoff prepared by Hudlow for actual storm conditions yielded remarkably good results since a point rainfall value was used in the simulation. The forecast for flood peak is really a probabilistic forecast and indicates the most probable peak based on antecedent rainfall and probable subsequent rainfall. Fig. 14 is an example of a forecast. The actual or observed peak was 500 cfs.

Testing rainfall synthesis by Monte Carlo methods. Although the streamflow forecast in Fig. 14 appears very good, it was felt that the entire procedure for synthesizing rainfall by Monte Carlo methods should be tested. Dale (1968), utilizing data for Ninnekah which was reserved for test purposes, has made a detailed study of the proposed method. His study did not attempt to reproduce the dry periods specifically; however, they could be recovered by the model with minor modifications. The selected procedure was to reproduce wet periods only and to test the suitability of these wet-period sequences as a prognostic technique.

Fig. 13 shows the probability of a wet hour given an increasing number of dry hours. The probability of a wet hour given six or more previous dry hours decreases monotonically to almost zero based on the 175 months of Huddle's study. Therefore, an hourly rainfall sequence can be considered essentially terminated after 6 hr.

In the study by Dale a wet period or storm was defined as a sequence of wet hours preceded by a period of six or more dry hours and followed by a period of six or more dry hours. This is illustrated with the rainfall bar graph in Fig. 15. The storm can have dry-hour sequences, of any length up to five, interspersed within the total length. A dry sequence of 6 hr terminates the storm, and any subsequent wet hours

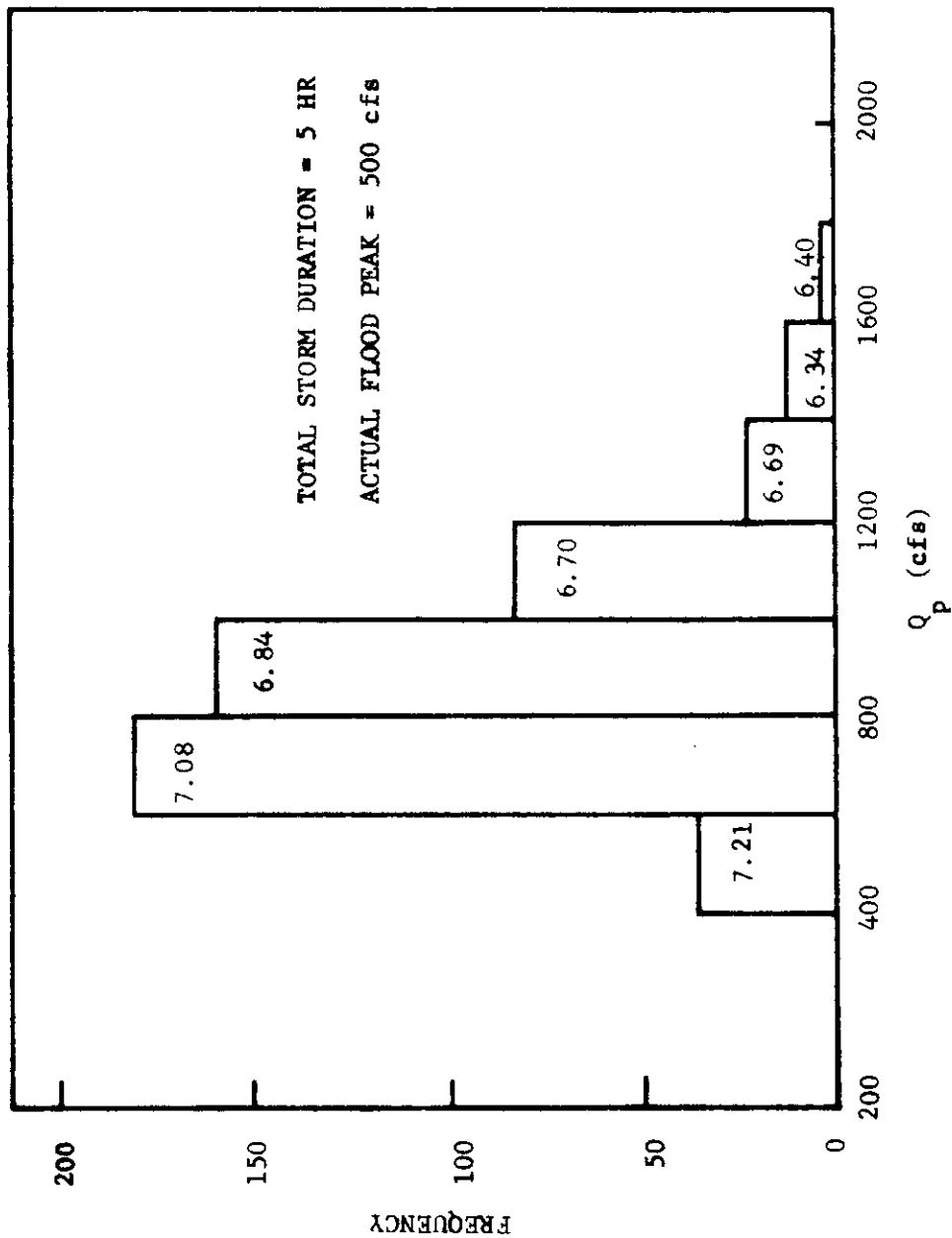


Fig. 14. Frequency histogram of hydrograph-peak discharges, as derived from the stochastic model (storm of May 9, 1965, 1st two hours of rainfall given). The numbers in the histogram are the average lag times determined for each class interval, in hours.

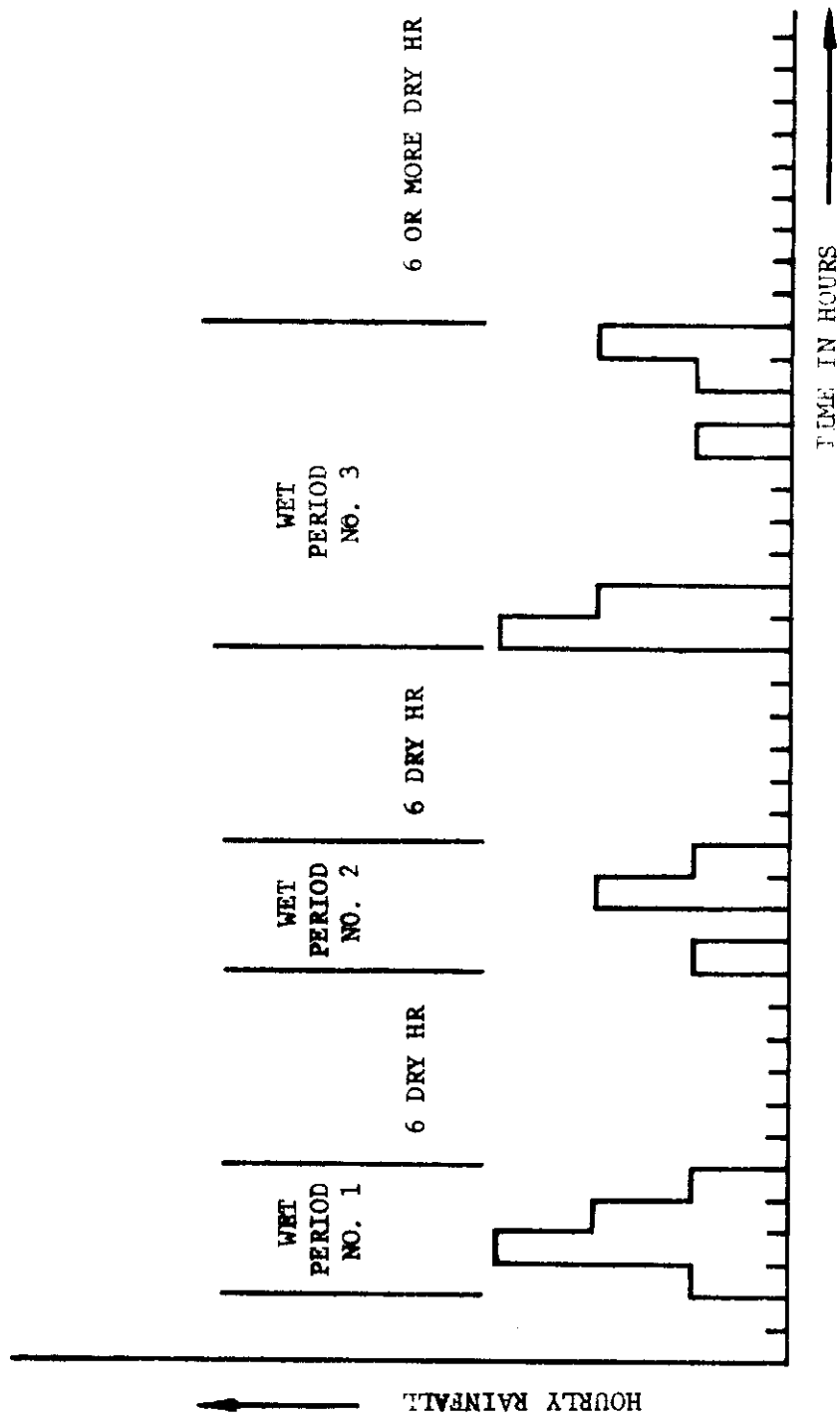


Fig. 15. Bar graph of hourly rainfall illustrating wet period lengths.

that are generated are considered as a separate storm.

Each storm was described in terms of the following characteristics:

- (1) total storm length in hours,
- (2) total wet hours, and
- (3) total storm rainfall in inches.

The generated storms were tested for each of the three parameters listed above. The actual historic storms were measured for the same parameters, and a comparison of the synthetic values to the actual values comprised a test of the modeling procedure.

The occurrence of a stochastic event can be defined in terms of probability, and the resulting probability distribution of a series of discrete random events then represents the likelihood of occurrence of that series of events. When hourly precipitation amounts are treated as such a series, the time pattern of the series values will be controlled by the probability distribution. If the distribution is constant with time, it is said to be stationary, and the probability of the occurrence of a specified amount of precipitation is the same at time  $(t)$  as at time  $(t + \Delta t)$ . A nonstationary distribution varies, continuously or discretely, throughout the process. Both distribution types may be used in a single process. This study used stationary probabilities within each synoptic type. The probabilities vary from one synoptic type to another.

The six synoptic types of this study describe the rainfall processes without regard to time of year or hour of the day at which the individual storms originate. The season, time of day, and synoptic type are all related to some extent. The season and hour of the day were not included in this study because of the limited data which were available.

Each day of the 33 months of test data (These data were reserved by Huddle (1967) from the original Ninnekah data for testing purposes.) was evaluated for occurrence of storms and synoptic type. All wet periods were considered as storms and identified with a synoptic system. The assignment of synoptic type was made by utilizing Daily Weather Maps published by the Weather Bureau. The procedure was partially subjective because some of the storms transited two daily maps. A

different synoptic type was often evident on succeeding maps, especially during periods of transit of warm, cold, or stationary fronts. Approximately 30 per cent of the test storms had some doubt as to accuracy of assignment. The time of day of storm onset was of use in some of these marginal assignments, particularly with regard to the squall-line type and the cold-front type.

The 78 selected storms include all cases, in the 33 available months, where a wet sequence was preceded or succeeded by six or more dry hours. Actual lengths varied from 1 hr to 27 hr.

The maximum length of time to operate the model in any particular synoptic pattern depends on the time period that each of the six synoptic types dominated the area. Determination of these lengths would be necessary for reproducing an entire historical record and was beyond the objectives of this study. The model must be operated for a period sufficient to determine an optimum length of each synthetic storm type.

There were three storms, of the 78 available, that were longer than 24 hr. Practical considerations limited the individual generated storm lengths to 29 hr. This was sufficient to represent all test storms and still retain a valid assumption of no change in synoptic type within the storm period. The design procedure does not indicate a direct test of the degree of validity of this assumption. The only cases of concern are the storms of extreme length where the initial synoptic classification is the most subjective. It is of interest to note that all but one of the test storms of length greater than 10 hr were of two types. These were the warm-front and the stationary-front.

The purpose of testing a model for rainfall synthesis is to ensure that the modeling procedure adequately describes the equivalent process observed in nature. No completely satisfactory testing procedure exists. An element of doubt will always exist as to whether a synthetic record can replace or exactly reproduce an historic one. Actual rainfall processes are complicated and not yet completely understood. It is not likely, therefore, that any model based on a simple hypothesis will be able to describe totally the actual process.

The best hypothesis would be one that considers all of the individual and interacting parts of the rainfall process. The adopted procedures of synthesis can be expected to reproduce only a few of the more important features of the rainfall record which has been compiled from a series of historic events. In some uses the satisfaction of one requirement implies the satisfaction of another not specifically mentioned. For this reason, several parameters have been selected as principal requirements of the synthesis, and if these are modeled adequately, the procedure is considered to be suitable.

In some situations the test results may indicate that the procedure of synthesis fails to produce acceptable results. It may be feasible then to determine the cause, and the consequences of failure may merely limit the scope of the applications of the synthetic data.

The generated storms were tested for each of three selected parameters: total hours, wet hours, and total rainfall. This was done by determining whether the frequency distribution of values of a given parameter were the same for both historic and synthetic data. A test which may be used is the Kolmogorov-Smirnov test (Siegel, 1956). The test can be applied as a one-sample test or a two-sample test. A one-sample test compares an observed distribution to a known or "fixed" distribution. If the known distribution is one of the parametric distributions, the test is considered a parametric test. The two-sample test is a test of whether two independent samples have been drawn from the same population or from populations with the same distribution. It is nonparametric and requires no knowledge about the true frequency distributions. The test is sensitive to any difference in the distributions of the samples such as central tendency differences, dispersion, skewness, etc. The two-tailed test measures these differences irrespective of direction. Only the absolute value of the differences of the two compared distributions is of concern. The one-tailed test is used to decide whether or not the values of the population from which one of the samples was drawn are stochastically larger than the values of the population from which the other sample was drawn. The one tailed test evaluates the prediction that the values of an experimental sample will be "better" than those of a control sample.

The two samples in this study would be, first, the historic parameter and, second, the synthetic parameter. If these two samples were drawn from the same population distribution then the cumulative distributions of both samples may be expected to be fairly close to each other and should show only random deviations from the population distribution. Any wide deviation from the distribution would suggest that the samples come from different populations and could be taken as evidence for rejecting the null hypothesis, which is that the two samples come from the same population.

The test is applied by deriving a cumulative frequency distribution of a given parameter using both historic and synthetic rainfall data.

The largest absolute difference between the step functions of the two distributions becomes the test statistic,  $D$ ,

$$D = \text{Maximum } | S_s(X) - S_h(X) |, \quad (28)$$

where  $S_s(X)$  is the cumulative frequency distribution for the synthetic data and  $S_h(X)$  is that for the historic data. The sampling distribution of  $D$  has been determined and the probabilities associated with the occurrence of values as large as an observed  $D$  under the null hypothesis have been tabled (Siegel, 1956). The application of the one-tailed test is identical except that we find the maximum value of  $D$  in a predicted direction, i.e.,

$$D = \text{Maximum } [ S_s(X) - S_h(X) ]. \quad (29)$$

The alternate hypothesis in the one-tailed test is that the population values from which one of the samples was drawn are larger than the population values from which the other sample was drawn.

The probability of rejecting the null hypothesis when it is true is the level of significance of the test, and for the case studies described later a value of 0.01 was used. Critical values for the Kolmogorov-Smirnov test vary with the sizes of the samples used. The sample size of each group of historic and synthetic sequences was random. The size was controlled partially, however, by the number of storms tested in a group. Sample values for both the historic and synthetic sequences must be divided into equal intervals; too few intervals tend to obscure the  $D$  value



of the cumulative step function. The test was applied to data grouped by synoptic type to obtain the largest number of intervals.

If two rainfall sequences can be shown to have the same measure of central tendency, even though their lengths differ considerable, then the two sequences can be accepted as being similar in their effect. For example, an historic rainfall sequence may be 5 hr long with a mean value of  $0.05 \text{ in. hr}^{-1}$ . Its synthetic counterpart may be 8 hr long with an average value of  $0.03 \text{ in. hr}^{-1}$ . Both storms would have the same approximate total rainfall. One storm may have all but a few hundredths of its rain in the first 3 hr. The second may have most of its rain in the last few hours or evenly distributed. The effect of both storms would be essentially the same. The result is that the three parameters used to describe each sequence may offset each other or reinforce each other. A test of the integrated effects of all parameters would be a more rigorous test of the relation between a synthetic and an historic sequence.

The Mann-Whitney U test (Siegel, 1956) may be used to test whether two independent groups have been drawn from the same population. It is one of the most powerful nonparametric tests and is essentially a median test. Two considerations in the selection of a statistical test are:

1. The efficiency of the test. A test which is least wasteful of data would have the highest efficiency (Hodges and Lehman, 1956).
2. The power of the test. This is a measure of the ability of the test to make an accurate decision (Spiegel, 1961).

Mood (1954), Hodges and Lehman (1956), and Witting (1960) investigated the efficiency of the Mann-Whitney U test in comparison with other parametric and nonparametric tests. Their conclusions were generally in agreement that the Mann-Whitney test had high efficiency for testing two samples of unequal length. Dixon (1954) has shown that rank sum tests have very high local power efficiency greater than 95 per cent for both large and small samples.

Consider two rainfall sequences each with a given number of wet hours of varying amounts. One is a synthetic sequence developed by some modeling process and will be called sample x. The corresponding historic sequence will be called sample y. The null hypothesis is that

a sample  $x$  from some population  $X$  does not differ a significant amount from sample  $y$  from population  $Y$ . This implies that  $X$  and  $Y$  have the same distribution. If the probability that  $x$  equals  $y$  is exactly one-half, then  $X$  equals  $Y$ . For a two-tailed test the alternate hypothesis is that  $P(x > y) \neq \frac{1}{2}$  which means that the "bulk" of population  $X$  is different from the bulk of population  $Y$  (Mann and Whitney, 1947). The amount that  $x$  differs from  $y$  depends on the significance level desired.

For illustration of the test procedure consider again two rainfall sequences. Sample  $x$  is an historic sequence  $n_1$  hr long and sample  $y$  is a synthetic sequence of length  $n_2$  hr, where  $n_1$  is smaller than  $n_2$ . To apply the  $U$  test we first combine the hourly amounts, observed or derived, from both groups, and rank these in order of increasing size. Algebraic size is considered in the ranking because the lowest ranks are assigned to the largest negative numbers. Of course, there are no negative values of hourly rainfall. Zero amounts representing dry hours in the sequence are assigned the lowest ranks. Now examine the  $x$  group with  $n_1$  hours. The value of the test statistic,  $U$ , is given by the number of times that an hourly value in the  $x$  group with  $n_1$  hours in the ranking. As an example, suppose an historical storm of 3 hr is compared with its synthetic counterpart which happens to be 4 hr long. Now  $n_1 = 3$  and  $n_2 = 4$ . Suppose the hourly amounts were (in inches)

x storm	0.01	0.04	0.06	
y storm	0.01	0.02	0.03	0.05

In order to find  $U$ , we first rank these values in order of increasing size, being careful to retain the identity of each value as either an  $x$  or  $y$  value:

0.01	0.01	0.02	0.03	0.04	0.05	0.06
x	y	y	y	x	y	x

Now consider the control group and count the number of  $x$  values that precede each  $y$  value. For the  $y$  value of 0.01, one  $x$  value precedes. The same is true of the 0.02  $y$  value and the 0.03  $y$  value. The 0.05  $y$  value is preceded by two  $x$  values. Thus  $U = 1 + 1 + 1 + 2 = 5$ . Either

group may be selected as the control group. When  $x$  is considered the control group, the value of  $U$  is then the number of  $y$  values that precede  $x$  values. From the given ranking this  $U$  is then  $0 + 3 + 4 = 7$ . There are two different  $U$ 's for any ranked sequence and  $U_1 + U_2 = n_1 n_2$ . The desired  $U$  is always the smaller of the two so that both must be calculated. Obviously  $U_1$  can be transformed from  $U_2$  by the formula

$$U_2 = n_1 n_2 - U_1 . \quad (30)$$

The sampling distribution of  $U$  under the null hypothesis is known; therefore, we can determine the probability associated with the occurrence, under the null hypothesis, of any  $U$  as extreme as an observed value of  $U$ . The probability values of  $U$  for various significance levels have been tabled (Siegel, 1956) and the only elements required to enter the tables are  $n_1$ ,  $n_2$ , a calculated  $U$ , and an accepted significance level. For this study a 0.01 significance level was used in order to obtain an equal significance to the other tests used in the study.

In the given example  $n_1 = 3$ ,  $n_2 = 4$ , and the smaller  $U = 5$ . The appropriate table indicates that the critical value of  $U$  for a significance level of 0.01 is zero. That is, the null hypothesis could not be rejected at the predetermined significance level unless  $U$  had been equal to zero. The observed  $U = 5$  had a probability of occurrence of 0.429. The conclusion is that the  $x$  and  $y$  values are well "mixed" and have almost the same median value. If the two group values were perfectly mixed, then  $U_1$  would equal  $U_2$  and the two samples would have the same median, implying that their respective populations have the same distribution. If all the  $x$  group values are either larger or smaller than all of the  $y$  group values, then the two  $U$  values would either be zero or  $n_1 n_2$ . In the example used,  $U_1$  would equal zero and  $U_2$  would equal 12. Since the smaller  $U$  is used to test for significance, there is no danger of focusing on the wrong group in obtaining the test statistic. In the case of maximum difference the  $U_1$  and  $U_2$  values it is seen that the  $x$  median and the  $y$  median would be farthest apart when there is no mixing of the hourly rainfall values. The conclusion would be that the population distributions are significantly different. The acceptable separation of the two samples depends on the desired significance level.

The Mann-Whitney U test assumes that the hourly rainfall amounts in the samples represent a distribution which has underlying continuity. Very precise measurement of a variable which has underlying continuity reduces the probability of a tie, between observed values, to zero. The relatively crude measurement of hourly rainfall values that are presently employed result in occurrences of ties.

The requirement of the model is that the first hour of both the historic and synthetic sequences have exactly the same quantity of precipitation. Any total number of dry hours in either sequence exceeding one will produce a tie. The tied scores are assumed to be different but the difference is simply too refined or minute for detection within the capability of measurement. When tied values occur, they are each assigned the average of the ranks they would have had if no ties had occurred. If the ties occur between two or more observations in the same group, the value of U is not affected. If ties occur between two or more observations involving both groups, the value of U is affected. The effect is usually negligible unless the lengths of the ties are quite long. Siegel (1956) states that a typical example had over 90 per cent of its values involved in ties but the effect on the test statistic was only two parts in 345 or 0.06 per cent increase in the U value computed. The recommendation is that ties should be corrected for only if the proportion of ties is very large (almost 100%), or if some of the tied runs are quite large. Even then, this correction should not be applied unless the observed probability of the obtained U value is very close to the previously set critical value for the chosen significance level.

A method of testing two comparative rainfall sequences for differences other than central tendency would be of additional value in deciding the success of the model. One test that can do this is the Wald-Wolfowitz runs test (Siegel, 1956). This test is applicable for testing the null hypothesis that two independent samples have been drawn from the same population against the alternative hypothesis that the two groups differ in any respect whatsoever. For sufficiently large samples the Wald-Wolfowitz test can reject the null hypothesis if the two populations differ in any way: in central tendency, in variability, in skewness, kurtosis, or whatever.

The rationale and method of applying the Wald-Wolfowitz test is identical, up to a point, to that of the Mann-Whitney U test. The ranking of two sample groups is identical. The test statistic  $r$  is obtained by observing the number of times the identities of the ranked values change. This is a different procedure than that used to calculate the U statistic, thus, the Wald-Wolfowitz "runs" test is independent of the Mann-Whitney "rank-sum" test. Now it can be reasoned that if two samples are from the same population, then the values of one sample will be well mixed with those of the other. This will be evinced by a large number of runs. When  $r$  is sufficiently small, the null hypothesis is rejected and the two samples will represent populations with different distributions. The exact type of difference that is tested can be determined only by inspecting the type and location of runs in a combined ranked sequence. The maximum value of this test can be utilized by combining it with the Mann-Whitney U test results. At a given significance level two comparative rainfall sequences have four possibilities of passing or failing both tests. these are:

- (1) pass both tests,
- (2) pass the U test, fail the  $r$  test,
- (3) fail the U test, pass the  $r$  test,
- (4) fail both tests.

The first and fourth cases are of no additional assistance as the same information would be gained by use of the U test alone.

Possibility (2) could be of value because two compared samples may pass the U test by having the same median but one sample may have significantly more variability than the other. The runs test would then reject the null hypothesis and a closer decision as to the type of difference can be made.

Possibility (3) is more difficult to apply. When two compared samples fail the U test by having different central tendencies they would almost certainly fail the runs test due to the same difference in the represented distributions. Examination of actual results discussed later indicates this to be the case. A positive evaluation of the runs test then can be made only in those cases where the U test is passed.

The most likely reason for the difficulty in applying the runs test is that it is not very good at guarding against accepting the null hypothesis erroneously with respect to any one difference tendency. This is called a Type II error and the power of a test is its ability to minimize Type II errors, i.e., to avoid making wrong decisions (Spiegel, 1961). The application used in this study should be of value as it allows the use of the runs test as an additional judgment to the Mann-Whitney U test.

The initial procedure that was adopted to obtain a representative synthetic sequence from a selected number of sequences was:

1. Generate a selected number of  $N$  synthetic sequences all with the same initial condition. The initial condition was obtained by use of the first hourly amount of a chosen historic sequence and the condition of the previous 5 hr.
2. Sum all the first-hour values and divide this sum by  $N$  to obtain a mean value for the first hour. The process was repeated for each succeeding hour. The resulting storm sequence is an arithmetic hourly average of  $N$  generated sequences.
3. Compare this averaged storm to the corresponding historical storm.
4. Increase the value of  $N$  and repeat steps 1, 2, and 3.
5. Evaluate the effect of increasing  $N$  on the three chosen parameters.

$N$  was initially assigned values of 10, 20, 50, 150, and 500. This nonlinear increase of  $N$  could possibly indicate a convergence of parameter values. Eighteen of the 78 actual storms were selected for test purposes to characterize the various lengths, synoptic types, and first-hour values. The initial conditions of each storm were used to generate an averaged synthetic storm.  $N$  synthetic sequences were generated for each of the 18 synthetic storms. The mean length ranged 12.1 hr for  $N = 10$  to 19.2 hr for  $N = 50$ . The significant result is that increasing  $N$  by a factor of 50 did not indicate convergence of storm lengths. Mean synthetic storm length for all  $N$  exceeded mean historical storm length by a factor of two to four. The other two parameters revealed similar values. Wet hour and total rainfall values exceeded their actual historic counterparts

by 50 to 100 per cent for all N. The preliminary conclusion was that no improvement would be achieved by increasing the number of simulations beyond the 20 to 100 range. Excessive parameter values, especially storm length, were a result of a number of long, wet, storm sequences in each simulation group.

With the above process a generated sequence of 29-hr length could have dry periods of six or more hours and yet contribute hourly rainfall amounts, in the later hours, sufficient to add excessive length to the average storm.

An effort was made to improve the simulation process in order to obtain a shorter, more realistic storm length. A storm was defined earlier as terminating after a sequence of six dry hours. The probability of a wet hour after six or more preceding dry hours is 0.005 (Table 7, row 1). If each storm sequence is examined after generation and then terminated when a 6-hr dry period is encountered, an improvement in the averaged sequence is noted. The hourly averaged storm of N modified storms showed a more realistic value of storm length. An additional modification was the conversion of any average hourly value less than 0.01 in. to zero. Amounts below 0.01 in. are not normally measurable so this is deemed justified. Another group of simulations with N varying from 10 to 150 revealed a considerable decrease in the length for all N values. No obvious trend of length with increasing N was found. The final adopted procedure was to obtain two types of synthetic sequences. The averaged sequence was the first one used and the lengths were not modified. This same distribution was then truncated as indicated above. This resulted in modification of all three parameters by decreasing the total length, wet hours, and total rainfall of the averaged sequence. Both the truncated sequence and the averaged sequence were tested separately against their corresponding historical sequences.

The testing procedures described earlier were used to compare the three parameters of each type of synthetic sequence to the three parameters of the corresponding historical sequence. The two-tailed Kolmogorov-Smirnov test was applied to each synoptic group of storms.

Synthetic sequences were generated using 20 and 100 simulations for each historic storm. Type 2 and type 3 storms were simulated 500 times. Table 9 depicts the maximum D values obtained for each parameter and simulation number for cold-front type storms. The one-tailed Kolmogorov-Smirnov test was performed simultaneously with the two-tailed test. The observed chi-square values are shown beneath the critical D values for each synoptic group in the tables. The critical chi-square ( $\chi^2$ ) value at a 0.01 significance level is 9.21. Probabilities of the observed chi-square values are shown in parentheses. The chi-square values determine the extent that the synthetic values are stochastically larger. The conclusion is that the model, as developed and modified, successfully produces rainfall sequences that do not differ significantly, at the 0.01 level, from actual short-and-medium length historic sequences. The percentages of storms of each type that passed the U test at the 0.01 significance level are depicted in Table 10. Percentage values obtained indicate marked success of the truncated averaged sequence in reproducing real rainfall sequences.

Table 11 depicts the results of the Wald-Wolfowitz runs test for the identical simulation runs of Table 10. Significant values of the test statistic  $r$  were available for the 0.05 level and the sequences were tested at that level. Test results indicated that a lower percentage of storms passed the runs test than passed the rank test. This is to be expected as the runs test evaluates all types of differences between the compared distributions. Siegel (1956) states, "When one rejects the null hypothesis on the basis of a test which guards against any kind of difference, one can then assert that the two groups are from different populations but one cannot say in what specific way(s) the populations differ." Application of the test results to rainfall sequences indicates that synthetic sequences with little or no difference in central tendency may have significant differences in variance or kurtosis. Relative magnitudes of the differences may be useful in evaluating the success of the modeling scheme. The runs test detected more sequences with different distributions than the rank test but does not say what these are.



Table 9. D and  $\chi^2$  values of selected characteristics of rainfall sequences for type 1 (cold front) storms

Critical  $\chi^2 = 9.21$

Selected Parameter	Improved Averaged Sequences		Truncated Averaged Sequence		Test Statistic
	N = 20	N = 100	N = 20	N = 100	
Total Length	0.129	0.129	0.144	0.153	D observed
	0.189	0.189	0.217	0.215	D critical
	4.93	4.97	4.66	5.28	$\chi^2$ observed
	(0.08)	(0.08)	(0.09)	(0.07)	
Wet Hours	0.166	0.116	0.137	0.145	D observed
	0.209	0.206	0.232	0.228	D critical
	6.68	3.34	3.75	4.26	$\chi^2$ observed
	(0.04)	(0.19)	(0.17)	(0.13)	
Total Rainfall	0.101	0.059	0.058	0.056	D observed
	0.203	0.206	0.215	0.217	D critical
	2.63	0.85	0.76	0.70	$\chi^2$ observed
	(0.28)	(0.66)	(0.69)	(0.70)	

Table 10. Percentage of storms passing the Mann-Whitney U test at a significance level of 0.01

Synoptic Type	Improved Averaged Sequence			Truncated Averaged Sequence		
	N = 20	N = 100	N = 500	N = 20	N = 100	N = 500
Cold Front	87	71	-----	100	96	-----
Warm Front	86	86	93	100	100	93
Stationary Front	100	69	77	100	92	92
Squall Line	80	80	-----	100	100	-----
Warm Air Mass	82	73	-----	100	100	-----
Cold Air Mass	55	36	-----	91	91	-----
Total All Types	81	69	85	99	96	92

Table 11. Percentage of storms passing the Wald-Wolfowitz runs test at a significance level of 0.05

Synoptic Type	Improved Averaged Sequence			Truncated Averaged Sequence		
	N = 20	N = 100	N = 500	N = 20	N = 100	N = 500
Cold Front	67	67	-----	75	75	-----
Warm Front	86	86	72	93	100	100
Stationary Front	69	38	46	69	62	85
Squall Line	60	80	-----	80	80	-----
Warm Air Mass	82	64	-----	91	82	-----
Cold Air Mass	45	18	-----	45	36	-----
<b>Total All Types</b>	69	59	59	76	73	93

Actual application of the synthetic sequences in some prescribed situation may require the user to evaluate the effect of differences in variance or Kurtosis. Success of the modeling scheme is based primarily on the test of central tendencies being most descriptive of any difference in the "effect" exerted by two compared rainfall sequences.

Tables 10 and 11 indicate that the highest degree of success was attained with the truncated averaged sequence using 20 simulations per storm.

The following conclusions were drawn concerning the rainfall simulation technique:

1. The sixth-order Markov chain appears to reproduce adequately the rainfall process for Ninnekah, Oklahoma.
2. The derived sequence utilizing a frequency modification with 20 simulations of each historic test storm gave the highest degree of success for this study.
3. Synoptic type 6 (cold air mass) sequences had the greatest disparity between synthetic and historic storms. A possible explanation for this may be the difficulty in defining the synoptic type. Hiser (1956) applied the same six types to precipitation patterns in Illinois. The climatology of Oklahoma may depart sufficiently from that of Illinois to require a separate set of synoptic types. Test storms and those sequences of Huddle's record which were designated as type 6 may, in fact, be of another type. All 11 test storms designated as type 6 occurred between November and April denoting a strong relation to type 1 storms. Type 6 storms usually occurred 24 to 36 hr after passage of a cold front at the surface. Cold front and cold air mass storms exhibit almost identical parameter characteristics.
4. Application of a stochastic model, as developed in this study, offers exceptional possibilities as a probabilistic forecasting method.
5. A number of transition probabilities were zero in the ten-by-ten matrices. There were insufficient sequences in the 175

months of record of Huddle's study to provide meaningful transition probabilities for all possible transitions.

6. Optimum operating time for the model is dependent on the application of the generated sequences. A general test of the stochastic probabilities requires synthesis of long sequences. The minimum period should be longer than the length of the longest available test storm or the length of the time period defined in the sixth-order modeling scheme.
7. Modification procedures developed in this study prevent the resulting weighted synthetic sequences from attaining extreme lengths. Existence of a significant number of actual extreme length storms requires a modification procedure adaptable to the longer storms. Adoption of the initial unmodified averaged sequence seems to offer promise as a long-storm synthesis method.

Comparison of conditional probabilities. In the development of the stochastic model for rainfall simulation conditional probabilities were determined for a single station, Ninnekah, Oklahoma. These probabilities were then applied to rainfall for specific areas of several square miles. Heaton (1968) has studied the variability of conditional probabilities for various rain-gage densities. For his study, a rainfall network maintained by the ARS over the Lowery Draw Watershed near Sonora, Texas, was selected.

The Lowery Draw Watershed (Fig. 16) contains 14 standard recording rain gages (weighing type) and has an area of 48 mi<sup>2</sup>. Slightly over 6 yr of continuous data were available from June 15, 1961 through June 31, 1967. There were a total of 178 storms ( $\geq 0.10$  in.) with a total of 2167 hr of precipitation during this period.

Areal averages of hourly precipitation were calculated using the Thiessen-polygon weighting method (Thiessen, 1911). Weighted average rainfall for the total area (for each clock hour of rainfall) then was calculated from

$$\text{Areal Precipitation} = \sum_{i=1}^n TW_i \times P_i, \quad (31)$$

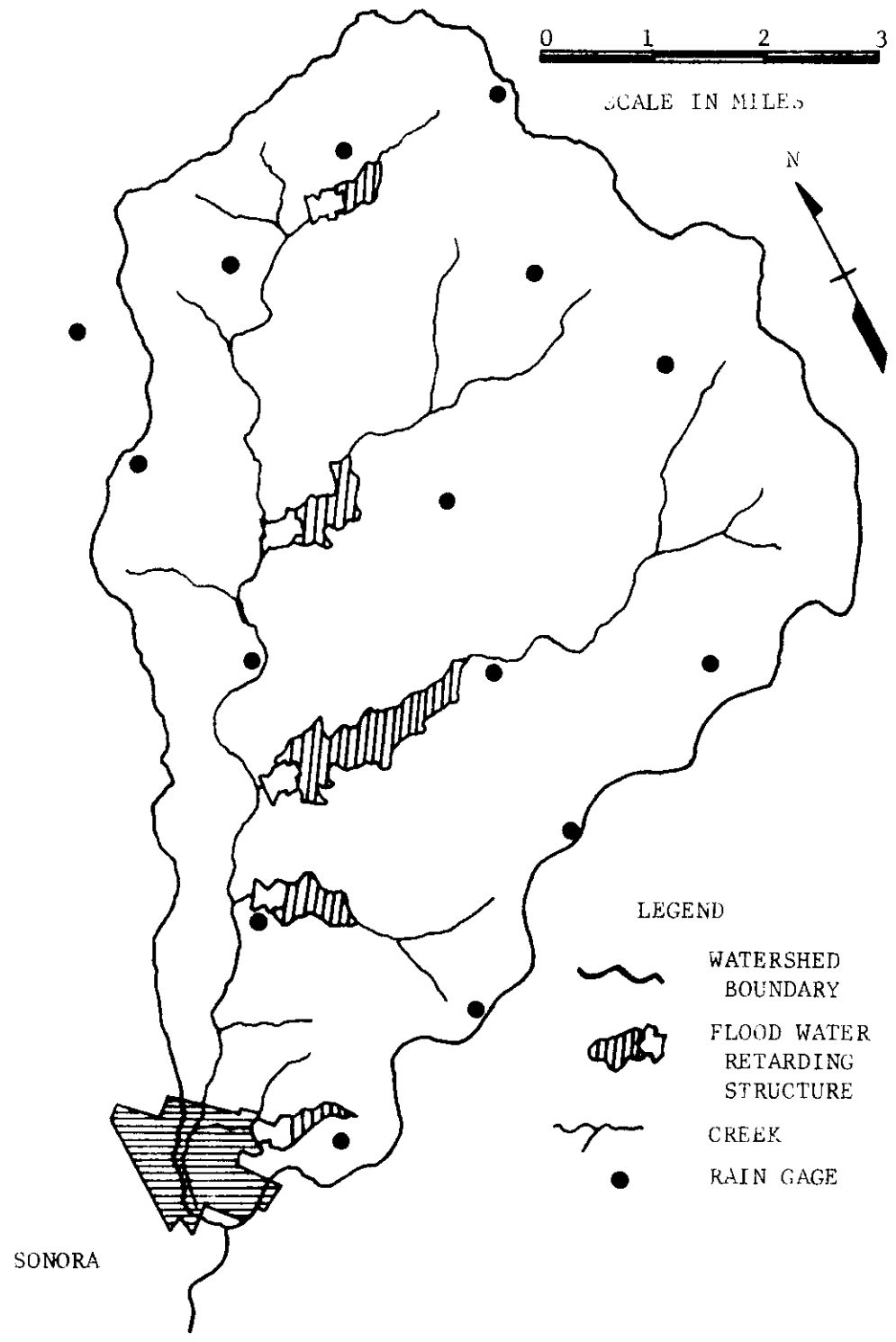


Fig. 16. Map of Lowery Draw Watershed.

where  $n$  is the number of rain gages used in the Thiessen-polygon pattern  $P_i$  is the precipitation measured at rain gage number  $i$ , and  $TW_i$  is the Thiessen weight of  $i$ . Thiessen-polygon patterns were prepared for 14 rain gages and for other networks of various density.

Areal averages for hourly and total-storm rainfall were calculated using the number of rain gages and average rain-gage densities indicated in Table 12.

Selection of the particular rain gages for inclusion in the various Thiessen-polygon patterns was made at random, in that the Thiessen patterns were constructed long before the actual data were examined. Some degree of subjectivity was involved in selecting the rain gages for inclusion in the less-dense patterns in that an attempt was made to obtain a somewhat uniform spatial distribution of the rain gages. In addition, two single rain gages were selected at random (one each from northern and southern portions of the basin) to be compared with the most-dense network.

For the area studied in Oklahoma the intensity and duration of precipitation appeared to vary with the synoptic situation producing the precipitation. As a result, precipitation was classified into six basic synoptic types corresponding to the synoptic situation from which they occur. It was observed, for the area concerned in the study by Heaton, that precipitation might be more suitably classified according to precipitation type. The three basic precipitation types which occur in west central and west Texas can be categorized as precipitation resulting from:

- (Type I) well-organized strong convective cloud systems (pre-cold frontal and squall line precipitation);
- (Type II) large-scale upslope motion (front south of station, i.e., warm front, stationary front, or cold air mass); and
- (Type III) isolated rain showers and thunderstorms (warm air-mass precipitation).

Each storm (and consequently each inclusive hour of precipitation) was assigned to one of the three types utilizing Daily Weather Maps,

Table 12. Number of gages used and corresponding gage densities

Number of Rain Gages Per 48 mi <sup>2</sup>	Average Rain-Gage Density (Mi <sup>2</sup> per Gage)
14	3.43
12	4.00
10	4.80
8	6.00
6	8.00
5	9.60
3	16.00



Weather Bureau, ESSA. Freezing precipitation, which comprised a very small percentage (approximately ten events in 6 yr of record) of the total data, was deleted from the records.

Precipitation in the United States is measured and recorded to the nearest hundredth of an inch. Since the amount of precipitation measured for a specific clock hour can vary from 0.00 in. to several inches (the hourly data for the Lowery Draw Watershed include several cases of hourly rainfall in excess of 3.00 in.), the number of possible amounts can be quite large. Calculations of conditional probabilities including all possible amounts of precipitation (graduated in increments of 0.01 in.) not only would be extremely tedious, but also would require periods of record much longer than currently available. An hourly rainfall of 0.31 in. is not significantly different from a rainfall of 0.36 in. (for practical purposes). Therefore, for the purposes of this study, precipitation amounts were grouped into ten classes, Table 13.

The frequencies of occurrence for each of the ten classes which followed a specified class were tabulated for the various rain-gage densities and precipitation type.

In order to compare the probability and frequency distributions of the less-dense networks (those having less than 14 rain gages) with those of the 14 rain-gage network, two significance tests were employed. The chi-square ( $\chi^2$ ) significance test (Siegel, 1956) was used to compare the frequency distributions for each of the precipitation types. When using the  $\chi^2$  test to compare two frequency distributions, the total number of observations in the two distributions must be equal. In order to meet this criterion, it was necessary to weight the total number of observations in each of the distributions based on the 14 rain gages to the sample distribution to which it was compared. Another of the criteria for use of the  $\chi^2$  test is that each expected class must have a frequency  $\geq 5$ . Therefore, it was necessary to combine (group) some of the adjacent classes in order to satisfy this criterion.

Since this study was not concerned with the probabilities of the ten possible classes following Class 1 (0.00 in.) precipitation and

Table 13. Classes of amounts of hourly precipitation

---

Class	Amount (in.)
1	0.00
2	trace ( $\leq 0.005$ in.)
3	0.01-0.02
4	0.03-0.06
5	0.07-0.10
6	0.11-0.20
7	0.21-0.30
8	0.31-0.40
9	0.41-0.70
10	$>0.70$

---

since the probability of a wet hour following a dry hour is very small, no attempt was made to compare these distributions. Because the number of occurrences of large precipitation amounts (Class 7 and larger) was relatively small, it also was necessary to group all Classes 7, 8, 9, and 10 into one new Class 7. This was done only for significance testing. The critical  $\chi^2$  values were those corresponding to  $(n - 1)$  degrees of freedom since the only constraint was that of stipulating the total number in the expected distribution. The results of the test are indicated in Table 14.

The Kolmogorov-Smirnov (K-S) test (Siegel, 1956) also was used to compare corresponding distributions for the three precipitation types. The K-S test determines the amount by which the cumulative distribution of one sample deviates from that of another. The maximum deviation "D" is then compared to the known "D" distribution. The K-S test for comparing distributions seems quite applicable for testing the distributions of this study for two reasons: (1) cumulative probability distributions are compared (recall that in the Markov process the cumulative distributions are used); and (2) the K-S test is applicable for any distribution. The results of the K-S test were nearly identical to those of the  $\chi^2$  test. It should be pointed out that the distributions that failed the K-S test (and  $\chi^2$ ) were most often those corresponding to the larger classes (the larger precipitation amounts).

The results of both the  $\chi^2$  and K-S tests indicate that there is a significant difference between the conditional probability distributions of point and areal amounts of hourly precipitation. In order to illustrate the variations and differences in the point and areal probability distributions calculated from this data, conditional probabilities ( $P_c$ ) versus precipitation class are plotted for each of the tested classes in Fig. 17. All of the three precipitation types were included in calculating the probabilities for Fig. 17. It can be seen from this figure that, in most cases, the probability of a dry hour following a wet hour using a single rain gage is much higher than the probability obtained using areal precipitation from 14 rain gages.

Table 14. Results of  $\chi^2$  test of frequency of distributions  
(Number failed / Total number tested)

No. of Rain Gages Per 48 mi <sup>2</sup>	TYPE I		TYPE II		TYPE III	
	LEVEL		LEVEL		LEVEL	
	.95	.90	.95	.90	.95	.90
1	4/6	4/6	5/6	5/6	4/6	4/6
3	3/6	5/6	2/6	2/6	4/6	4/6
6	1/6	1/6	1/6	2/6	1/6	2/6
8	0/6	0/6	0/6	0/6	0/6	0/6

Frequency distributions derived from networks having >8 rain gages were found to be not significantly different from the distributions based on 14 rain gages.

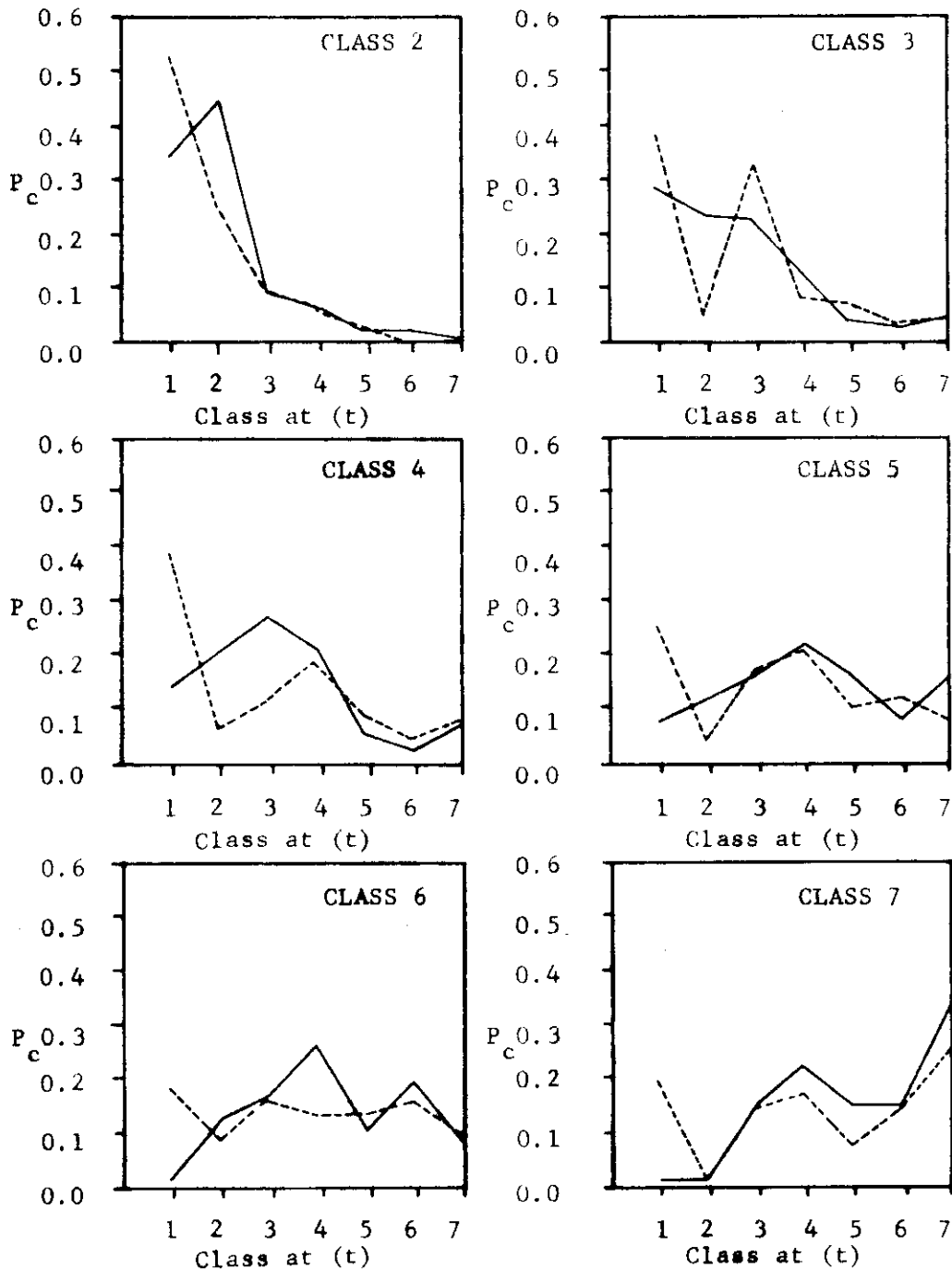


Fig. 17. Single (dashed line) and 14 rain-gage (solid line) distributions of conditional probabilities for all precipitation types.

It is apparent, then, that further work is required in the development of the model for rainfall-runoff simulation. Certainly a prime consideration is a better system for the determination of conditional probabilities for areal rainfall.

## HURRICANE BEULAH

### General

The hurricane-tornado has long been worthy of professional attention. Only recently, as the public became weather conscious and the density of data improved, has the importance of this hurricane-induced phenomenon been realized. Beulah's 141 tornadoes (September 19 through September 23, 1967), which were over five times greater in number than the previous record of 26, dramatically illustrated the importance of the hurricane-induced tornado and the need for further investigation.

The objectives of this study were to determine the temporal and spatial distribution of the tornadoes associated with hurricane Beulah, relate the large number of occurrences to existing atmospheric conditions, and advance a theory as to the possible cause of the tornadoes (Grice, 1968).

Hurricane Beulah began as a disturbance on the intertropical convergence zone off the African Coast on August 28, 1967. The disturbed area moved westward with little intensification until September 4 when a weak circulation was found by reconnaissance aircraft. Early on September 5 the existence of a weak depression was verified by ship reports indicating the center of the disturbance to be located near 14.0°N, 57.0°W.

Beulah reached tropical storm strength on September 7 when an investigating aircraft reported winds of 40 mph and a central pressure of 1006 mb. At this time, the center was 20 mi off the west coast of Martinique and was causing rains as great as 12 in. per 18 hr to fall over the northern Windward Islands.

Beulah strengthened rapidly as it moved northwestward and attained hurricane intensity shortly after midday on September 8, thus becoming the third September storm of this century to achieve hurricane force in the eastern Caribbean. Beulah continued to develop as it moved northwestward toward the Dominican Republic and Haiti. However, these two

countries escaped most of Beulah's fury when the storm changed to a more westward track.

From September 10-13 Beulah weakened considerably, due primarily to a confluent jet stream to the rear of a 200-mb trough which was positioned over the storm, thus impeding its outflow. During this period the central pressure rose about 55 mb and winds decreased from 150 mph to only 40 mph.

As the confluent jet aloft moved eastward and was replaced by a ridge, Beulah intensified again into a hurricane and began a north-westward course toward Cozumel Island and the Yucatan Peninsula. Landfall on Cozumel occurred during the evening of September 16 with wind speeds about 100 mph. Late on the morning of the 17th Beulah crossed the Yucatan Peninsula and into the Gulf of Mexico. Weakened little by its trip across Cozumel and Yucatan (pressure rise of 10 mb and a wind decrease of 25 mph) and being nourished by the warm waters of the Gulf of Mexico, Beulah became a large and dangerous hurricane. On September 19 reconnaissance recorded a central pressure of 923 mb, second only to the 920 mb found in hurricane Hattie in 1961.

Beulah moved toward the north-northwest, making landfall at about daybreak on September 20 between Brownsville and the mouth of the Rio Grande. Shortly before moving inland Beulah's winds were estimated at 160 mph. The Weather Bureau Office at Brownsville recorded a peak gust of 109 mph; however, the anemometer shaft was tilted about 30°, therefore, the actual wind speed was higher. The SS Shirley Lykes, which was anchored at Port Brownsville, reported winds of 136 mph with the passage of the hurricane.

Beulah continued her northwestward heading after moving inland. This movement carried the center of the storm to the east of Brownsville and Harlingen to about 40 mi south of Alice where Beulah decreased to tropical storm intensity shortly after 1800 CST on September 20. During the next twelve hours, the tropical storm made a series of loops about 60 mi southwest of Corpus Christi, Texas, before drifting to the southwest and dissipating in the mountains near Monterrey, Mexico. Gale force winds (winds equal to or greater than 39 mph) affected all of

southern Texas south of a line from just north of San Antonio to just north of Houston. Data from Mexico were not sufficient to determine the affected areas to the west; however, it is quite probable that locations as far as Monterrey experienced winds of gale force.

Hurricane winds (winds equal to or greater than 75 mph) covered an extensive area, extending outward 50 to 75 mi from the storm center. Again, the data in Mexico were insufficient to determine the areal extent of strong winds in that country; however, by interpolation it appears hurricane force winds occurred as far south as 24°N.

The precipitation which fell during the passage of Beulah (September 19 - September 23) is shown in Fig. 18. Of primary interest are the two areas of maximum precipitation located 70 mi northwest of Brownsville (BRO) and 40 mi north of Corpus Christi (CRP). The maximum near Brownsville coincides fairly well with the hurricane's path; however, the area near Corpus Christi is about 100 miles north of the northernmost point reached by Beulah. From a comparison of various hurricanes and the associated precipitation patterns presented by Schoner and Molansky (1956), it appears that for a hurricane to have an area of maximum precipitation a relatively large distance from the hurricane's path there needs to be a lifting mechanism such as a front, orographic barrier, or low-level confluent wind field. There were no fronts or confluent wind fields close to the area and although it is possible for the orographic features to have a slight effect, it is highly unlikely that the 700 ft rise from the coast to San Antonio could cause the second maximum area. Consequently, there must be another explanation for the second maximum precipitation area; this reason will be discussed later.

#### Tornadoes Associated With Beulah

In compiling the number of tornadoes associated with hurricane Beulah, tornado reports gathered from teletype data and a survey made by the Office of the State Climatologist, Weather Bureau, ESSA, were used. After the list of tornadoes was compiled, the occurrences were grouped into 3-hr periods (0000-0259 CST, etc.) and the data for each



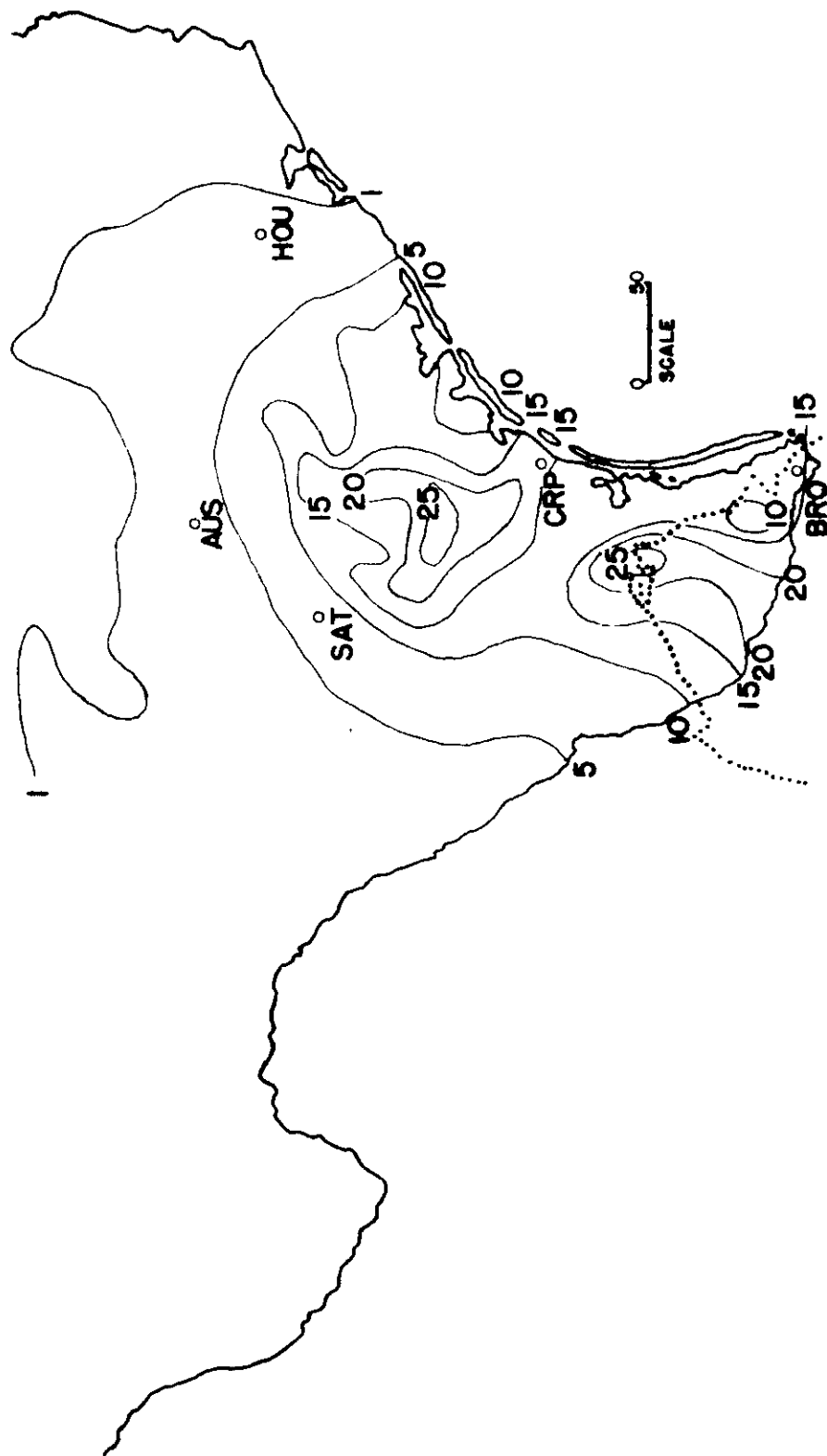


Fig. 18. Total precipitation (inches), September 19 - September 23, 1967.

period plotted on a single map. This was done not only to provide a suitable time breakdown but to provide also a means whereby duplicate reports of tornadoes could be determined. This procedure made it necessary to use only those tornadoes for which times of occurrence were given; this criterion eliminated 7 tornadoes. It should be emphasized at this point that although the utmost caution was used in determination of the reported number of tornadoes and since it is quite possible that unobserved tornadoes occurred over the Gulf of Mexico and between populated areas, the figure of 141 tornado occurrences quoted in this investigation is probably a minimum value.

Daily and areal distributions. About 90% of the 141 tornadoes reported during the period September 19 through September 23 occurred from September 20 through September 22 with about 45% of the total occurring on September 20. The daily distribution of tornado occurrences is given below:

Sept 19	Sept 20	Sept 21	Sept 22	Sept 23
8	62	33	33	5

Since the largest number of tornadoes occurred on September 20 and generally decreased afterward, it would appear that, to a certain extent, the number of tornadoes varied with the intensity of the hurricane and, consequently, the strength of the wind field.

It could not be determined whether there was a large number of occurrences on the 19th since the hurricane was in the Gulf of Mexico; however, it does not appear likely in view of the probable causes for the tornadoes which will be discussed later.

The area of Texas affected by the tornadoes was large, extending north from near Brownsville to the Dallas-Fort Worth area and as far east as Beaumont. However, the largest percentage occurred in an area bounded by Corpus Christi, San Antonio, Austin and Houston. There were no tornadoes reported in Mexico.

On September 19 the tornadoes were scattered from northeastern to southern Texas with no general pattern except for the small cluster located near Victoria. On September 20 the tornadoes occurred primarily in a band about 85 mi wide which extended from the coast near Palacios through Victoria to northwest of Austin and San Antonio. The tornadoes

which occurred during the 21st were confined generally to within 100 mi of the coast. Most of the tornadoes on September 22 were centered around Corpus Christi in a small area 80 mi long and 60 mi wide. Within this small area, 29 separate tornadoes were reported.

An item of particular interest was the tornado pattern of September 20. The eastern boundary of the tornado area appeared as a distinct, clear line; whereas, the western boundary was ill defined. That is, the tornadoes on the eastern boundary occurred along a line; but, those near the western boundary showed no such pattern. For lack of a better description, this pattern was designated as a "straight line pattern." This "straight line pattern," although not as distinct, could be detected also on September 21 along a line from Beaumont to north of Houston to about half way between Houston and San Antonio. Since the tornadoes on September 22 occurred over such a small area, it could not be determined whether or not this peculiar pattern was present.

An investigation was performed to determine the relationships in time and space between the tornadoes and Beulah. Of the 141 tornadoes reported, 103 could be directly associated with the movement and other features of Beulah. The remaining 38 occurred on September 22 and 23 when Beulah was poorly organized and located in the mountains near Monterrey, Mexico, thus making it impossible to obtain any accurate information on the storm. However, with various assumptions, the 33 tornadoes of September 22 also were included.

To determine if the occurrence of the tornadoes was time dependent, the grouped data were plotted against time. The results are shown in Fig. 19. One hundred nine or about 78% of the tornadoes occurred between 0600 CST and 1800 CST, with a preferred time between 0900 CST to 1200 CST. This is in relatively good agreement with the results of Smith (1965) who stated that the most favorable time period was from 0300 CST to 1500 CST. Pearson (1966) suggested that a reporting bias exists for daylight hours since tornadoes are usually sighted by the general public. It is probable that there is a reporting bias for daylight hours in the tornadoes associated with Beulah; however,

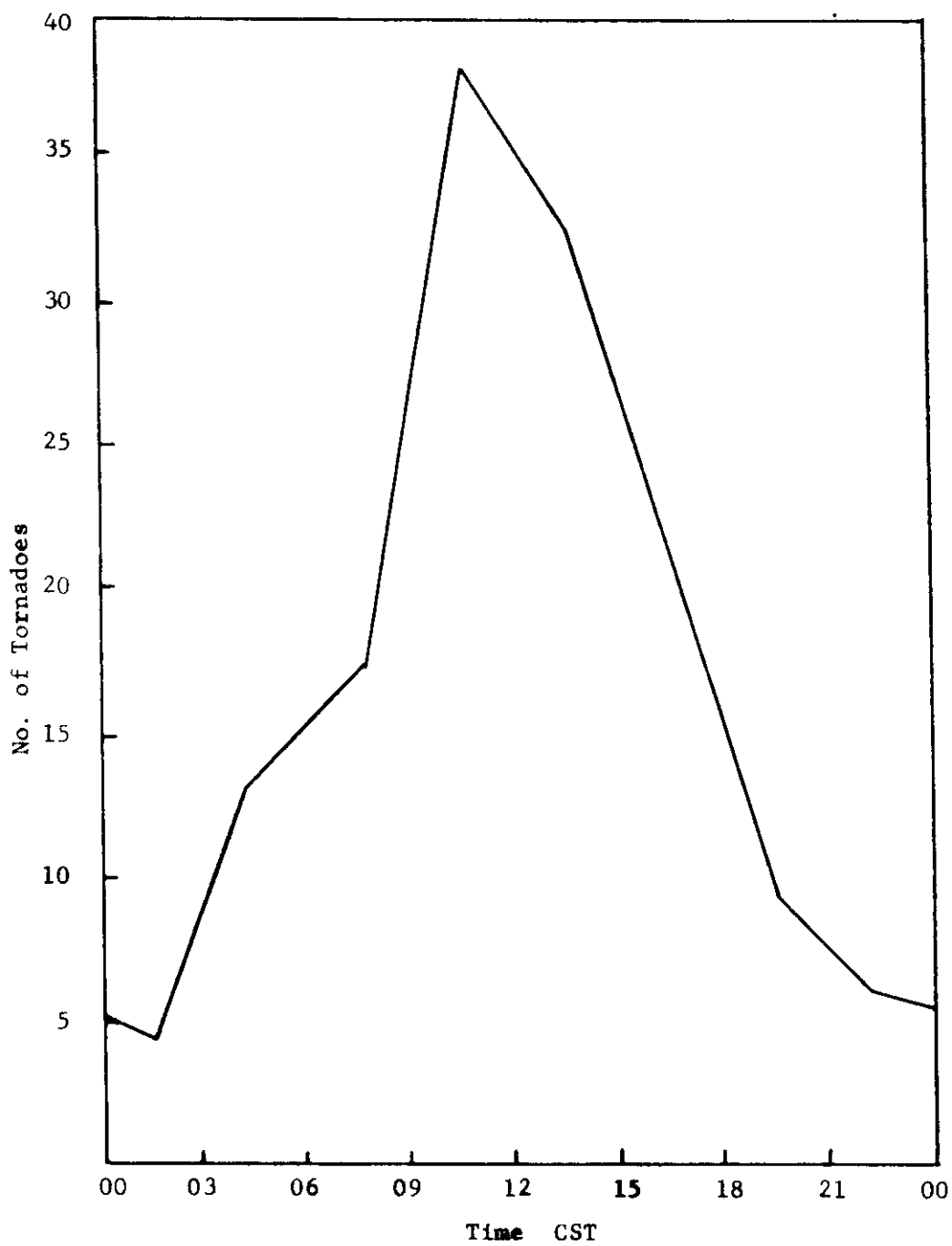


Fig. 19. Relation of tornado occurrence to time of the day.

it seems very unlikely that the large difference between daylight and night hours can be accounted for by reporting preference.

An examination was made to determine if the tornadoes preferred a particular quadrant of the hurricane in relation to the storm's motion. It was found that 42% of the tornadoes favored the first quadrant measured clockwise from the hurricane's direction of movement; the second quadrant had 25% of the occurrences, the third 15%, and the fourth 8%. Ten per cent occurred when the storm was stationary.

Beulah's movements during tornado occurrence were very different from the movement of the previous hurricane studies, e.g., Hill *et al.* (1966). Out of 101 tornadoes, nearly 65% occurred during southwest, west, or northwest headings, directions which should be least favorable to tornado formation.

Beulah's path in only one respect resembled Smith's (1965) path of the "tornado-producing hurricane model," i.e., both had northwesterly trajectories just before landfall. In all other respects they differ. The direction of movement of Beulah after landfall was different from what might have been expected. Smith's model requires an immediate recurvature from primarily a northwest course before moving inland to a northeast course overland. Beulah had a northwestward movement before and about 100 mi after crossing the coast. However, she then curved toward the southwest, the reverse of Smith's model.

Several additional relationships were surveyed for pertinent results. The first was the relation of the tornadoes to the gale force winds. It was found that 101 of the 141 tornadoes, or about 72%, occurred outside the area of gale force winds. Although no firm conclusion can be made, it appears upon examination of other hurricanes and associated tornadoes that this high percentage is unusual.

A plot of the tornado locations was made to determine if a relationship exists between the number of occurrences and distance of the hurricane from shore; no significant results were found. The tornadoes were checked as to their distance from the eye of the hurricane. It was found that 64 of the 103 tornadoes occurred at a distance of 165 mi to 285 mi.

### Possible Cause of the Tornadoes

The occurrence of 141 tornadoes associated with a hurricane is a highly unusual event. However, there were several other features of Beulah and her tornadoes which definitely were not ordinary. The two widely separated areas of maximum rainfall which occurred with this storm are unusual when compared with the one general area of maximum rainfall found with most hurricanes. The "straight line pattern" exhibited along the eastern borders of the tornado areas on September 20 and September 21 was very peculiar. Most important, the distribution of the tornadoes when compared with distributions of other hurricane-induced tornadoes indicated unusual relations with respect to quadrant and semicircle of greatest frequency, direction of hurricane movement, and gale force winds.

Since there were so many tornadoes with Beulah and since their distributions were somewhat different from the distributions of other hurricane tornadoes, it would appear that the factors which normally cause hurricane-induced tornadoes may have been intensified greatly with Beulah. These factors or synoptic conditions also could have caused the second area of maximum precipitation and the "straight line pattern" of the tornadoes on September 20 and September 21.

During the period September 19-22, 1967, a high pressure area covered the southeastern United States and the Gulf of Mexico. Soundings showed the atmosphere to be stable along the Gulf Coast east of Texas although there were no temperature inversions observed. Drier air was observed along the Gulf Coast east of Texas and was probably associated with the extension of the high pressure area over the Gulf of Mexico south and east of the Texas Coast. Subsidence associated with the high could account for the presence of the dry air.

The leading edge of the dry air appeared to be advected inland along the Texas and Louisiana coasts particularly on September 20 and 21, 1967. On both days, the air over Victoria and Lake Charles was drier at 1800 CST than at 0600 CST at the 700-mb level. The wind direction was south to southeast at all altitudes below 400 mb during the entire period. Variations in the magnitude of the subsidence associated with

the high pressure area could have been partly responsible for the variation observed at these locations. The movement of the drier air inland along the coast might produce effects similar to an overrunning cold front in that the stability would be decreased below the level of the driest air, while above this level the dry air could cause lifting of the moist air.

The intrusion of dry air suggested above might account for many of the irregularities connected with Beulah and the associated tornadoes, viz.:

- (1) The large number of tornadoes could be explained by the lifting and the decrease in stability which occurred near the leading edge of the dry tongue;
- (2) Variation in the degree of dryness, the depth of the dry air and the slope of the discontinuity surface separating the moist and dry air masses could account for the second area of maximum precipitation. The rate of horizontal advection could have been partially responsible; however, the scarcity of wind data prevents a definite conclusion.
- (3) The "straight line pattern" exhibited by tornadoes on September 20 and September 21 was probably caused by lifting and a decrease in stability at the leading edge of the dry-air intrusion;
- (4) Since the location of the tornadoes depended on the location and movement of the dry air, it can be seen why the distributions of these occurrences failed to agree with the distributions of other hurricane-induced tornadoes; and,
- (5) The time preference exhibited by the tornadoes on September 20 and 21 could be accounted for by the variability in the intrusion of the dry air. Large numbers of tornadoes developed when drier air was advected from over the Gulf to over Texas.

The first question that would become apparent concerning the influence of dry air intrusion on the formation of tornadoes is: Could dry air near a hurricane be the reason for tornado formation and, if so, why did Beulah have a larger number than other storms?

To give a partial answer, the conditions surrounding hurricane Carla (September 1961) were examined. An area of dry air was found to exist to the northeast of Carla which was the quadrant of the storm in which the tornadoes formed. However, examination of the 500 mb dewpoint gradient revealed that the gradient with Beulah was about twice as large as the gradient with Carla. This could be the reason that Beulah had a larger number of tornadoes than Carla.

#### Conclusions

The following conclusions were inferred from this study:

- (1) The tornadoes associated with Beulah exhibited many characteristics which were unusual when compared with other hurricane-induced tornadoes. These included the preferred quadrant and semicircle of occurrence, hurricane heading during tornado formation, and relation of tornado occurrence to gale force winds.
- (2) The tornadoes were dependent not only on the parent cyclone, but apparently also on the dry air which was located near the tornado area.
- (3) From conclusion (2) the peculiarities of the tornadoes, which otherwise cannot be accounted for, may be explained.
- (4) It is highly probable that the formation of hurricane-tornadoes is related to the presence of dry air near the tropical cyclone, and the number of occurrences dependent on the strength and orientation of the wind field and the moisture gradient existing between the moist and dry air.

#### TABLES OF PRECIPITABLE WATER AND VERTICAL VARIATION OF TEMPERATURE

The hydrometeorologist is frequently confronted with the problem of the theoretical determination of precipitable water for various layers of the atmosphere. At the same time he may be interested in the vertical distribution of temperature. Tables were prepared several years ago by the Hydrometeorological Section, Weather Bureau (1951),



in the English system of units for a saturated pseudoadiabatic atmosphere. Although a relatively simple problem, conversion from the English to the metric system can often be tedious and frequently leads to errors in computation. Similar tables have been computed by Powers (1967) and Lehle (1968) for the metric system of units. Tables 15 and 16 are examples of the tables prepared for the variation of precipitable water and temperature with elevation. The range of temperatures used in the computations was for a sea level (1000 mb) temperature range from 5°C to 29°C and for an elevation range from sea level to 15,000 m for the precipitable water tables and to 10,000 m for the vertical variation of temperature.

As an example: If the sea level dewpoint temperature is 20°C and the air is saturated with a pseudoadiabatic lapse rate, the air will hold 42.1 mm of precipitable water between sea level and 4,000 m (see Table 15). The temperature at 4,000 m will be 0.9°C (from Table 16). The values in Table 15 are cumulative. If the precipitable water is required between 2,000 m and 4,000 m for the same condition, the incremental value will be  $42.1 - 27.2 = 14.9$  mm, where the value 27.2 mm is the total precipitable water between sea level and 2,000 m.

Table 15

DEPTH OF PRECIPITABLE WATER (MM) BETWEEN 1000-MB SURFACE AND  
INDICATED HEIGHT (M) ABOVE 1000-MB AS A FUNCTION OF 1000-MB TEMPERATURE  
(C) IN A SATURATED ATMOSPHERE WITH PSEUDOADIABATIC LAPSE RATE

HEIGHT (METERS)	TEMPERATURE (C) AT 1000-MB						
	19	20	21	22	23	24	25
50	0.8	0.9	0.9	1.0	1.0	1.1	1.2
100	1.6	1.7	1.8	2.0	2.1	2.2	2.3
150	2.4	2.6	2.7	2.9	3.1	3.3	3.5
200	3.2	3.4	3.6	3.9	4.1	4.3	4.6
250	4.0	4.2	4.5	4.8	5.1	5.4	5.7
300	4.8	5.1	5.4	5.7	6.1	6.4	6.8
350	5.5	5.9	6.2	6.6	7.0	7.5	7.9
400	6.3	6.7	7.1	7.5	8.0	8.5	9.0
450	7.0	7.5	7.9	8.4	8.9	9.5	10.1
500	7.7	8.2	8.7	9.3	9.9	10.5	11.1
550	8.5	9.0	9.6	10.2	10.8	11.5	12.2
600	9.2	9.7	10.4	11.0	11.7	12.4	13.2
650	9.9	10.5	11.2	11.9	12.6	13.4	14.2
700	10.5	11.2	11.9	12.7	13.5	14.3	15.2
750	11.2	12.0	12.7	13.5	14.4	15.3	16.2
800	11.9	12.7	13.5	14.3	15.3	16.2	17.2
850	12.6	13.4	14.2	15.2	16.1	17.1	18.2
900	13.2	14.1	15.0	15.9	17.0	18.0	19.2
950	13.9	14.8	15.7	16.7	17.8	18.9	20.1
1000	14.5	15.4	16.4	17.5	18.6	19.8	21.1
1050	15.1	16.1	17.2	18.3	19.4	20.7	22.0
1100	15.7	16.8	17.9	19.0	20.2	21.5	22.9
1150	16.3	17.4	18.6	19.8	21.0	22.4	23.8
1200	16.9	18.1	19.2	20.5	21.8	23.2	24.7
1250	17.5	18.7	19.9	21.2	22.6	24.1	25.6
1300	18.1	19.3	20.6	21.9	23.4	24.9	26.5
1350	18.7	19.9	21.2	22.6	24.1	25.7	27.3
1400	19.2	20.5	21.9	23.3	24.9	26.5	28.2
1450	19.8	21.1	22.5	24.0	25.6	27.3	29.0
1500	20.3	21.7	23.2	24.7	26.3	28.1	29.9
1600	21.4	22.9	24.4	26.0	27.8	29.6	31.5
1700	22.5	24.0	25.6	27.3	29.2	31.1	33.1
1800	23.5	25.1	26.8	28.6	30.5	32.5	34.7
1900	24.4	26.1	27.9	29.8	31.8	33.9	36.2
2000	25.4	27.2	29.0	31.0	33.1	35.3	37.7
2100	26.3	28.1	30.1	32.2	34.4	36.7	39.1
2200	27.2	29.1	31.1	33.3	35.6	38.0	40.5
2300	28.1	30.0	32.2	34.4	36.7	39.2	41.9
2400	28.9	31.0	33.1	35.5	37.9	40.5	43.2
2500	29.7	31.8	34.1	36.5	39.0	41.7	44.5
2600	30.5	32.7	35.0	37.5	40.1	42.9	45.8
2700	31.2	33.5	35.9	38.5	41.2	44.0	47.0
2800	32.0	34.3	36.8	39.4	42.2	45.1	48.2
2900	32.7	35.1	37.6	40.3	43.2	46.2	49.4
3000	33.4	35.8	38.4	41.2	44.1	47.3	50.5
3250	35.0	37.6	40.4	43.3	46.4	49.8	53.3
3500	36.5	39.2	42.2	45.3	48.6	52.1	55.8
3750	37.8	40.7	43.8	47.1	50.6	54.2	58.2
4000	39.0	42.1	45.3	48.7	52.4	56.2	60.4

TEMPERATURE (C) AS A FUNCTION OF HEIGHT (METERS) ABOVE 1000 MB  
 TEMPERATURE AT 1000 MB IN A SATURATED ATMOSPHERE  
 WITH A PSEUDOADIABATIC LAPSE RATE

HEIGHT (METERS)	TEMPERATURE (C) AT 1000 MB						
	19	20	21	22	23	24	25
100	18.6	19.6	20.6	21.6	22.6	23.6	24.6
200	18.1	19.1	20.2	21.2	22.2	23.2	24.2
300	17.7	18.7	19.7	20.8	21.8	22.8	23.8
400	17.2	18.3	19.3	20.3	21.4	22.4	23.4
500	16.8	17.8	18.9	19.9	21.0	22.0	23.0
600	16.3	17.4	18.4	19.5	20.5	21.6	22.6
700	15.9	16.9	18.0	19.1	20.1	21.2	22.2
800	15.4	16.5	17.6	18.6	19.7	20.8	21.8
900	15.0	16.0	17.1	18.2	19.3	20.4	21.4
1000	14.5	15.6	16.7	17.8	18.9	19.9	21.0
1100	14.0	15.1	16.2	17.3	18.4	19.5	20.6
1200	13.6	14.7	15.8	16.9	18.0	19.1	20.2
1300	13.1	14.2	15.4	16.5	17.6	18.7	19.8
1400	12.6	13.8	14.9	16.0	17.2	18.3	19.4
1500	12.2	13.3	14.5	15.6	16.7	17.9	19.0
1600	11.7	12.9	14.0	15.2	16.3	17.4	18.6
1700	11.2	12.4	13.6	14.7	15.9	17.0	18.2
1800	10.7	11.9	13.1	14.3	15.4	16.6	17.8
1900	10.3	11.5	12.6	13.8	15.0	16.2	17.3
2000	9.8	11.0	12.2	13.4	14.6	15.7	16.9
2100	9.3	10.5	11.7	12.9	14.1	15.3	16.5
2200	8.8	10.0	11.3	12.5	13.7	14.9	16.1
2300	8.3	9.5	10.8	12.0	13.2	14.4	15.7
2400	7.8	9.1	10.3	11.6	12.8	14.0	15.2
2500	7.3	8.6	9.8	11.1	12.3	13.6	14.8
2600	6.8	8.1	9.4	10.6	11.9	13.1	14.4
2700	6.3	7.6	8.9	10.2	11.4	12.7	13.9
2800	5.8	7.1	8.4	9.7	11.0	12.3	13.5
2900	5.3	6.6	7.9	9.2	10.5	11.8	13.1
3000	4.7	6.1	7.4	8.8	10.1	11.4	12.6
3100	4.2	5.6	6.9	8.3	9.6	10.9	12.2
3200	3.7	5.1	6.4	7.8	9.1	10.5	11.8
3300	3.2	4.6	5.9	7.3	8.7	10.0	11.3
3400	2.6	4.1	5.4	6.8	8.2	9.5	10.9
3500	2.1	3.5	4.9	6.3	7.7	9.1	10.4
3600	1.6	3.0	4.4	5.8	7.2	8.6	10.0
3700	1.0	2.5	3.9	5.4	6.8	8.2	9.5
3800	0.5	1.9	3.4	4.9	6.3	7.7	9.1
3900	-0.0	1.4	2.9	4.4	5.8	7.2	8.6
4000	-0.6	0.9	2.4	3.8	5.3	6.7	8.2
4100	-1.2	0.3	1.8	3.3	4.8	6.3	7.7
4200	-1.8	-0.2	1.3	2.8	4.3	5.8	7.2
4300	-2.3	-0.8	0.8	2.3	3.8	5.3	6.8
4400	-2.9	-1.3	0.2	1.8	3.3	4.8	6.3
4500	-3.5	-1.9	-0.3	1.3	2.8	4.3	5.8
4600	-4.1	-2.4	-0.8	0.7	2.3	3.8	5.4
4700	-4.7	-3.0	-1.4	0.2	1.8	3.3	4.9
4800	-5.3	-3.6	-1.9	-0.3	1.3	2.8	4.4
4900	-5.9	-4.2	-2.5	-0.9	0.8	2.3	3.9
5000	-6.5	-4.8	-3.1	-1.4	0.2	1.8	3.4

## APPENDIX A

PROJECT RELATED REPORTS, PUBLICATIONS, AND PAPERS

Hudlow, Michael D., "Techniques for Hydrograph Synthesis Based on Analysis of Data from Small Drainage Basins in Texas," Tech. Rep. No. 3, Water Resources Institute, Texas A&M Univ., 79 pp., May 1966.

Johnson, Odell M., "Applicability of Radar Observations to the Prediction of Storm Runoff," M.S. Thesis, Texas A&M Univ., 37 pp., May 1967.

Huddle, John P., "A Stochastic Technique for Synthesis of Hourly Precipitation," M.S. Thesis, Texas A&M Univ., 39 pp., May 1967.

Hudlow, Michael D., "Streamflow Forecasting Based on Statistical Applications and Measurement Made with Rain Gage and Weather Radar," Tech. Rep. No. 7, Water Resources Institute, Texas A&M Univ., 110 pp., August 1967.

Clark, Robert A., "Tropical Rainfall," paper presented at the XIV General Assembly of the International Union of Geodesy and Geophysics, Lucerne, Switzerland, October 1967.

Clark, Robert A., "Determination of Probable Maximum Precipitation Values in Tropical Regions," Proceedings of the Fifth Conference on Hurricanes and Tropical Meteorology, Caracas, Venezuela, November 1967 (in press).

Clark, Robert A., "Application of Weather Radar to Streamflow Forecasting and Reservoir Operations," Proceedings of the 12th Annual Water for Texas Conference, College Station, Texas, November 1967.

Runnels, R. C., "On the Feasibility of Precisely Measuring the Properties of a Precipitating Cloud with a Weather Radar," Tech. Rep. No. 10, Water Resources Institute, Texas A&M Univ., 118 pp., December 1967.

Dale, Walter M., "Synthesis of Hourly Rainfall by a Monte Carlo Method Using a Sixth-Order Markov Chain," M.S. Thesis, Texas A&M Univ., 81 pp., May 1968.

Heaton, Larry R., "An Investigation of the Variability of Rainfall Statistics Over a Small Area with Varying Rain-Gage Density," M.S. Thesis, Texas A&M Univ., 48 pp., May 1968.

Hudlow, Michael D. and Clark, Robert A., "The Feasibility of Using Radar Measurements in the Synthesis of Flood Hydrographs," Proceedings of the 13th Radar Meteorology Conference, Montreal, Quebec, p. 412-415, August 1968.

Runnels, Robert C., Moyer, Vance E., and Clark, Robert A., "Uncertainties in the Measurement of Liquid-Water Content Using the Gain-Step Technique," Proceedings of the 13th Radar Meteorology Conference, Montreal, Quebec, p. 388-391, August 1968.

Hudlow, Michael D. and Clark, Robert A., "Hydrograph Synthesis by Digital Computer," J. Hydraulics Div., ASCE, May 1969 (in press).

Grice, Gary K., "An Investigation of the Tornadoes Associated with Hurricane Beulah," M.S. Thesis, Texas A&M Univ., 38 pp., August 1968.

Hudlow, M. D., Clark, R. A., Dale, W. M., and Heaton, L. R., "Streamflow Forecasting Based on Statistical Applications and Measurements Made with Weather Radar," paper presented at Conference on Water Resources Engineering, ASCE, New Orleans, La., February 1969.

## REFERENCES

- Beers, Y., Introduction to the Theory of Error, Addison-Wesley, Reading, Massachusetts, 66 pp., 1957.
- Byers, H. R., Elements of Cloud Physics, Univ. of Chicago Press, Chicago, 191 pp., 1965.
- \_\_\_\_\_, and Braham, R. R., The Thunderstorm, United States Government Printing Office, Washington, 287 pp., 1949.
- Chow, Ven Te, Handbook of Applied Hydrology, McGraw-Hill, New York, 1420 pp., 1964.
- Crawford, N. H. and Linsley, R. K., "The Synthesis of Continuous Streamflow Hydrographs on a Digital Computer," Tech. Rep. 12, Dept. of Civil Engineering, Stanford Univ., 121 pp., 1962.
- Dale, Walter M., "Synthesis of Hourly Rainfall by a Monte Carlo Method Using a Sixth-Order Markov Chain," M.S. Thesis, Texas A&M Univ., 81 pp., May 1968.
- Dixon, W. J., "Power Under Normality of Several Nonparametric Tests," The Ann. of Math. Stat., 25(3):610-614, Sept. 1954.
- Fletcher, H. N., The Physics of Rainclouds, Cambridge Univ. Press, Cambridge, England, 386 pp., 1962.
- Greene, D. R., Clark, R. A., and Moyer, V. E., "3.2-cm Attenuation Related to Rainfall Rate and Liquid-Water Content," Proceedings of the Twelfth Conference on Radar Meteorology, Norman, Oklahoma, Oct. 1966.
- Grice, Gary K., "An Investigation of the Tornadoes Associated with Hurricane Beulah," M.S. Thesis, Texas A&M Univ., 38 pp., August 1968.
- Griffiths, J. F., private communication, Texas A&M Univ., 1967.
- Hartman, Monroe A., Ree, William O., Schoof, Russel R., and Blanchard, Bruce J., "Hydrologic Influences of a Flood Control Program," J. Hydraulics Div., ASCE, 93(3):17-25, May 1967.
- Heaton, Larry R., "An Investigation of the Variability of Rainfall Statistics Over a Small Area with Varying Rain-Gage Density," M.S. Thesis, Texas A&M Univ., 48 pp., May 1968.
- Hill, E. L., William Malkin and W. A. Schulz, Jr., "Tornadoes Associated with Cyclones of Tropical Origin-Practical Features," J. App. Met., AMS, 5, 745-763, 1966.
- Hiser, Homer W., "Type Distribution of Precipitation at Selected Stations in Illinois," Trans. Am. Geophys. Union, 37(4):421-424, August 1956.
- Hodges, J. L. Jr. and Lehmann, E. L., "The Efficiency of Some Nonparametric Competitors of the t-test," The Ann. of Math. Stat., 27(2):324-335, June 1956.
- Huddle, John P., "A Stochastic Technique for Synthesis of Hourly Precipitation," M.S. Thesis, Texas A&M Univ., 39 pp., May 1967.

- Hudlow, Michael D. and Clark, R. A., "Hydrograph Synthesis by Digital Computer," J. Hydraulics Div., SCE, May 1969 (in press).
- \_\_\_\_\_, "Streamflow Forecasting Based on Statistical Applications and Measurement Made with Rain Gage and Weather Radar," Tech. Rep. No. 7, Water Resources Institute, Texas A&M Univ., 110 pp., August 1967.
- \_\_\_\_\_, "Techniques for Hydrograph Synthesis Based on Analysis of Data from Small Drainage Basins in Texas," Tech. Rep. No.3, Water Resources Institute, Texas A&M Univer., 79 pp., May 1966.
- Hydrometeorological Section, Weather Bureau, "Tables of Precipitable and Other Factors for a Saturated Pseudo-Adiabatic Atmosphere," Weather Bureau Tech. Rep. No. 14, Washington, D.C. 27 pp., 1951.
- Tehle, William O., Unpublished Manuscript, Texas A&M Univ., 1968.
- Johnstone, Don, and Cross, William P., Elements of Applied Hydrology, The Ronald Press Company, New York, p. 229, 1949.
- Kessler, E., "Kinematical relations between wind and precipitation distributions," J. Met., AMS, 16(6):630-637, December, 1959.
- Laurenson, E. M., "A Catchment Storage Model for Runoff Routing," J. of Hydrology, 2:141-163, 1964.
- \_\_\_\_\_, "Hydrograph Synthesis by Runoff Routing," Rep. No. 66, Water Research Lab., The Univ. of New South Wales, 248 pp., 1962.
- Linsley, R. K., Kohler, M. A., and Paulhus, J. L. H., Hydrology for Engineers, McGraw-Hill, New York, 340 pp., 1958.
- Mann, H. B. and Whitney, D. R., "On a Test of Whether One of Two Random Variables is Stochastically Larger Than the Other," The Ann. of Math. Stat., 18(1):50-60, March 1947.
- Minshall, Neal E., "Predicting Storm Runoff on Small Experimental Watersheds," J. Hydraulics Div., ASCE, 86(8):17-38, August 1960.
- Mood, A. M., "On the Asymptotic Efficiency of Certain Nonparametric Two-Sample Tests," The Ann. of Math. Stat., 25(3):514-521, Sept. 1954.
- Parzen, Emanuel, Modern Probability Theory and Its Applications, John Wiley & Sons, Inc., New York, pp. 128-147, 1960.
- Pattison, Allan, "Synthesis of Hourly Rainfall Data," Water Resources Research, 1(4):489-498, 1965.
- \_\_\_\_\_, "Synthesis of Rainfall Data," Tech. Rep. No. 40, Dep. of Civil Engineering, Stanford Univ., 143 pp., July 1964.
- Pearson, Allen D., "Hurricane-Induced Tornadoes--A Review," American Society for Oceanography, Publication Number One, 114-131, 1966.
- Powers, Robert J., Unpublished Manuscript, Texas A&M Univ., 1967.
- Probert-Jones, J. R., "The radar equation in meteorology," Quart. J. Roy. Met. Soc., 88(378):485-495, October, 1962.

- Runnels, R. C., "On the Feasibility of Precisely Measuring the Properties of a Precipitating Cloud with Weather Radar," Tech. Rep. No. 10, Water Resources Institute, Texas A&M Univ., 118 pp., December 1967.
- Schoner, R. W. and S. Molansky, "Rainfall Associated with Hurricanes (and Other Tropical Disturbances)," National Hurricane Research Project, 3, 305 pp., 1956.
- Schreiber, H. R. and Kincaid, D. R., "Regression Models for Predicting On-Site Runoff from Short-Duration Convective Storms," Water Resources Research, 3(2):389-395, 1967.
- Sharp, A. L., Gibbs, A. E., Owen, W. J., and Harris, G., "Application of the Multiple Regression Approach in Evaluating Parameters Affecting Water Yields of River Basins," J. of Geophys. Research, 65(4): 1273-1286, April 1960.
- Siegel, S., Nonparametric Statistics, McGraw Hill, New York, 312 pp., 1956.
- Smith, John S., "The Hurricane-Tornado," Monthly Weather Review, 93, 453-459, 1965.
- Snyder, Franklin F., "Synthetic Unit-Graphs," Trans. Am. Geophys. Union, 19(I):447-454, 1938.
- Soil Conservation Service, Engineering Handbook, Hydrology, Sup. A, Sect. 4: U.S. Dep. of Agr., Washington, D.C., pp. 3.15-1 to 3.15-7, 1957.
- Spiegel, M. R., Theory and Problems of Statistics, Schaum, New York, 359 pp., 1961.
- Thiessen, A. H., "Precipitation for Large Areas," Mo. Wea. Rev., 39:1082-1084, July 1911.
- Wilson, E. B., Jr., An Introduction to Scientific Research, McGraw-Hill, New York, 375 pp., 1952.
- Witting, H., "A Generalized Pitman Efficiency for Nonparametric Tests," The Ann. of Math. Stat., 31(2):405-414, June 1960.